We are thankful to the three reviewers for their thoughtful comments and suggestions. We have revised the manuscript accordingly. Listed below are our point-by-point responses in blue to each reviewer's comments.

Response to Reviewer #1

Comments:

This manuscript describes atmospheric submicron aerosol sources and processes based on a field on-line measurement at an altitude of 260 nm in polluted Beijing, China, along with a comparison with an in-situ ground measurement. China has been suffering from serious air pollution issues, mainly due to complex and unclear vertical-dependent chemical and physical processes of atmospheric aerosols, although the ground-based characterization has been relatively well understood. This manuscript is well-written and provides some new and interesting data sets for understanding ambient primary and secondary organic aerosol sources and processes above an urban canopy. I strongly believe those results can make some important implications for atmospheric chemistry and physics community, and even for understanding the mechanism of haze formation in China. I recommend this paper can be published in ACP after addressing a few minor areas as follows.

We thank the reviewer's positive comments.

1. A five-factor solution for source apportionment of organic aerosol was chosen in this study, which includes three primary factors (FFOA, COA, and BBOA), and two secondary factors (LO-OOA, and OOA). The FFOA factor here involves fossil fuel combustion sources relative to traffic and coal combustion. This should be reasonable since it could not be separated even by HR-AMS PMF approach. To further support this reasonable factor of FFOA, did the authors try to check the ratio range between FFOA and delta CO (measured total CO minus background CO) at the ground site, as

comparing with any previous results (e.g., HOA+CCOA vs delta CO)? Another way to check this factor, it might be possible to constrain HOA and CCOA factors only for HR-AMS data using external reference mass spectra from previous studies at the same sampling site (e.g., Sun et al., 2016 ACP). Then, the authors could make an evaluation for unconstrained FFOA and constrained HOA+CCOA.

Good points. It is very challenging to separate the traffic-related HOA from coal combustion OA (CCOA) although Sun et al. (2016) was able to separate HOA from CCOA by using PMF analysis of high resolution mass spectra and the UMR spectra to m/z = 350. The reasons include: (1) very similar spectral patterns between HOA and CCOA at m/z < 120; (2) very similar temporal variations and diurnal cycles; (3) limited sensitivity of the ACSM, particularly for m/z's > 50 with large uncertainties in ion transmission efficiencies. As the reviewer mentioned, the ME-2 analysis of HR-AMS by constraining HOA and CCOA factors for OA spectra might be a choice to check FFOA. However, constraining HOA and CCOA in ME-2 may introduce new ambiguities to the OA source apportionment considering the reasons above. Although they are forced to be separated, the accurate concentrations of HOA and CCOA are difficult to be evaluated. In this study, we further tried to extend the PMF solution of the HR-AMS to 6 or 7 factors, but it is difficult to obtain more interpretable and meaningful solutions, moreover, HOA and CCOA are still not separated. Without additional measurements, the 5-factor solution of HR-AMS might be a safer choice.

Following the reviewer's suggestions, we compared the ratios between FFOA and delta CO at the ground site with those reported in previous studies. FFOA/ΔCO ranges from 0.1 to 9.9 (on average 1.9) in this study, which is lower than those during November 2011 to January 2012 (1.0−27.6, on average 7.1) (Sun et al., 2013), and January 2013 (0.1−37.8, on average 8.0) (Sun et al., 2014) at the same sampling site. But it is close to that observed in Zhang et al. (2016) in December 2014 (on average 2.7). These results suggest that the FFOA/ΔCO ratios might have significant variability year by year. Another reason is that the measurements in this study were

conducted at 260 m, which might have large differences from those at ground sites.

2. Generally, ambient oxygenated organic aerosol (OOA) derived from the AMS/ACSM PMF (or ME-2) approach includes a subset of oxidized organic aerosol factors (e.g., less or more oxidized OOA). Why did not the authors use a term of MO-OOA for your "OOA" factor, as explained in page 9 lines 25-26 "…indicating that OOA was more oxidized than LO-OOA"? (I guess it might be ok if just following the f44-f43-based criteria).

Thanks the reviewer's suggestion. Such an OOA factor is typically called as MO-OOA in previous studies. However, our recent study (Sun et al., 2016a) showed that higher f_{44} (fraction of *m/z* 44 in OA) does not necessarily correspond to higher oxygen-to-carbon (O/C) ratio. Also, this OOA factor was better correlated with nitrate than sulfate in our study, which is generally different from previous findings that MO-OOA was better correlated with sulfate. Therefore, the second SOA factor was named as OOA rather than MO-OOA to avoid confusions.

3. Page 9, lines 29-31 and page 10 lines 1-5. These are an interesting finding. The authors found that LO-OOA may be a kind of SOAs from combustion-related source(s), which has a good correlation with chloride and CO, respectively. The LO-OOA concentration at 260 m can be two times higher than that at ground site during some periods. Are these able to explain that the observation at 260 m could be closer to combustion-related SOA plumes/favorable heights rather than ground site? On the other hand, does this make sense to explain the rapid transformation of partial POA into LO-OOA (freshly formed SOA) due to processes of evaporation, oxidation and/or re-condensation (Robinson et al., 2007 Science) during transports from ground levels?

Thank the reviewer's comments. Yes, our results showed that LO-OOA was more easily formed at higher heights (e.g., 260 m) during the polluted periods with higher RH and coal combustion emissions (e.g., NHP and HP1). As the reviewer pointed out,

one reason is that aerosols at 260 m are subject to more influences from regional transport, and the other reason is that the higher RH and lower *T* at 260 m facilitate the gas-particle partitioning. However, it is very challenging to conclude that the differences of LO-OOA between 260 m and ground site are caused by evaporation, oxidation and/or re-condensation processes during the vertical transport. One major reason is the difficulties to separate the relative contributions of regional transport and vertical transport from ground site to LO-OOA at 260 m. Despite this, the reviewer suggested a very good point which should be addressed in future studies by conducting the continuously vertical measurements (from ground to 260 m) using one aerosol mass spectrometer.

4. Page 22, Figure 1: Some RH peaks at the ground level are much higher than at 280 m, e.g., October 14-20 and Nov. 02-09, as well as some similar peaks in heating periods, but air temperature is almost same. Is it possible to find any evidence about the enhancement of SOA productions due to aqueous-phase chemistry during these typical cases, with a comparison between ground and 260 m dataset?

Good points. We carefully checked the NR-PM_1 mass concentrations and fractions during the typical periods with much higher RH at ground level than 260 m to investigate the vertical differences and SOA formation process.

Although the nighttime RH at ground level was higher than that at 260 m during the measurement period in Fig. R1, the concentrations of SOA (LO-OOA + OOA) are consistently lower than those at 260 m. We are expecting more aqueous-phase processing at ground site due to higher RH. However, the higher SOA at 260 m suggests that there could be more important factors influencing the vertical differences. We did observe large increases in OOA and sulfate during Ep5 with the highest RH, indicating that aqueous-phase processing might be important for this episode. However, the aqueous SOA factor cannot be resolved from OOA with PMF or ME-2 analysis. This is also consistent with the fact that OOA in this study was better correlated with NO_3 than SO_4. Another reason is the average nighttime RH at

ground site was typically below 60%, and as a result, liquid water content was not high enough for strong aqueous-phase processing.

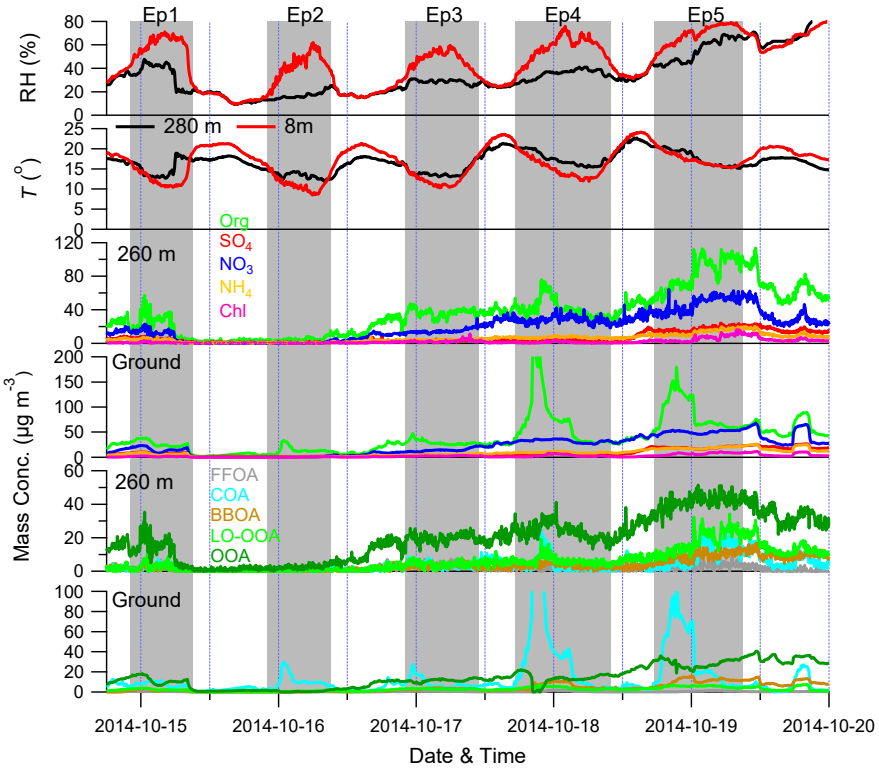

Figure R1. The time series of meteorological conditions (RH and *T*), NR-PM_1 species and OA factors both at ground and 260 m during 14 October to 20 October. Five episodes with much higher RH at ground level than 260 m are marked in dark grey.

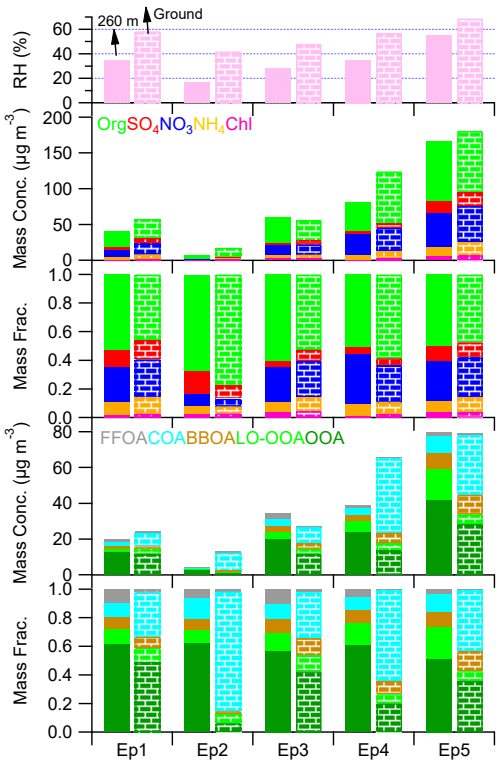

Figure R2. Average RH, mass concentrations and fractions for NR-PM_1 species and OA factors at ground level and 260 m during the five episodes marked in Fig. R1.

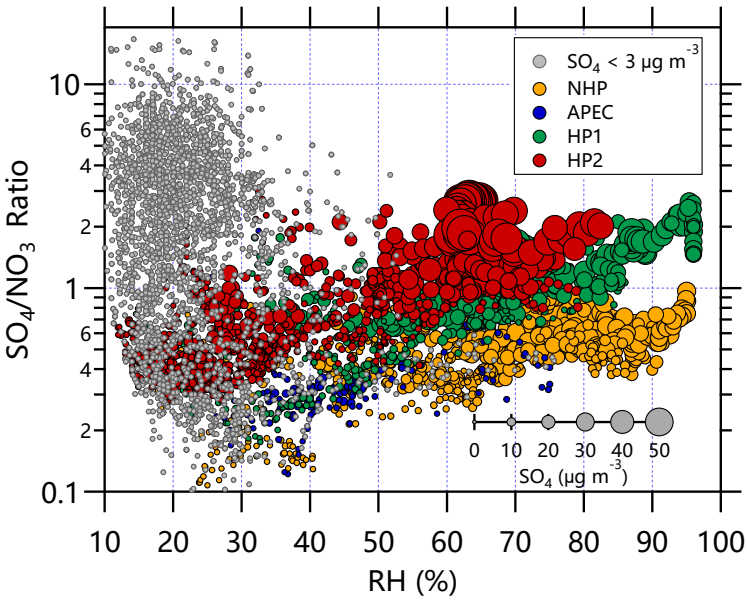

Figure 3: The variations of SO_4/NO_3 ratios as a function of RH during four different periods, i.e., NHP, APEC, HP1, and HP2. The marker sizes indicate the SO_4 concentrations, and the data points with the SO_4 concentrations less than 3 μg m^{-3} are marked in grey.

5. Page 24, Figure 3: What are the data points size-scaled by?

Thanks the reviewer for pointing this out. The data points were sized-scaled by the mass concentrations of sulfate (SO_4). The data points with SO_4 less than 3 μg m^{-3} are marked in grey. We revised this figure in the new version of the manuscript as shown above.

6. Page 26, Figure 5 (left panel): The factors of FFOA, COA, and BBOA were identified using the constrain mode (a-value), but LO-OOA and OOA were resolved using the PMF free mode. So, to be more directly clear for readers, the authors may consider adding the corresponding label in each mass spectrum of POA factors (e.g., constrained or a specific a-value) and SOA factors (e.g., unconstrained or free).

Good points. We revised Figure 5 as below.

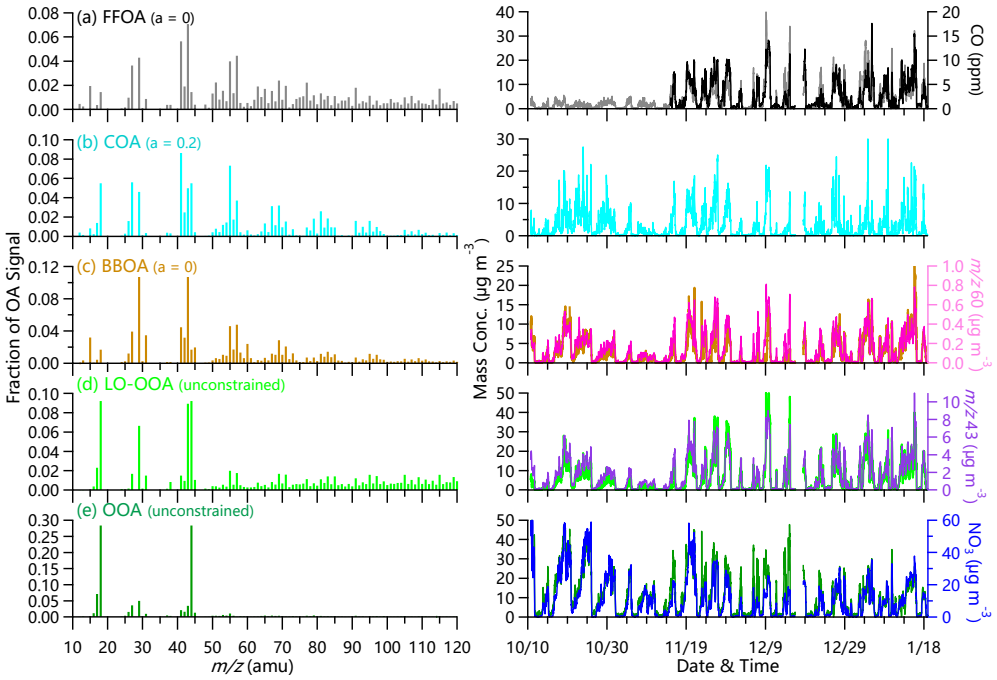

Figure 5: Mass spectra (left panel) and time series (right panel) of five organic aerosol (OA) factors including (a) fossil fuel-related OA (FFOA), (b) cooking OA (COA), (c) biomass-burning OA (BBOA), (d) less oxidized oxygenated OA (LO-OOA), and (e) oxygenated OA (OOA). Also shown in the right panel are the time series of tracers including CO, nitrate, *m/z* 60, and *m/z* 43.

7. Supplement: Pages 5-6, Figure S3 (d and e): Since LO-OOA and OOA factors were resolved by the PMF free mode, whereas FFOA, COA, and BBOA were constrained. The authors may highlight that the specific a-value is for constrained POA factors, but not for unconstrained SOA factors in both LO-OOA and OOA mass spectra.

We thank the reviewer for these suggestions. We revised the caption of Figure S3 to make the figure more clear for the readers. Now it reads:

"Figure S3: Mass spectra (left panel) and time series (right panel) of five organic aerosol (OA) components resolved at 260 m by ACSM using multi-linear engine 2 (ME-2): (a) fossil fuel-related OA (FFOA), (b) cooking OA (COA), (c) biomass-burning OA (BBOA), (d) low-oxidized oxygenated OA (LO-OOA), and (e) oxygenated OA (OOA). The 4-factor solution of PMF result was also shown here. Note that the mass spectra of two SOA factors in (d) and (e) were unconstrained, and the a values refer to those of three POA factors (i.e., FFOA, COA and BBOA)."

Response to Reviewer #2

General comments:

This manuscript reports results obtained during a measurement campaign undertaken at Beijing between October 2014 and January 2015. The authors deployed an Aerodyne ACSM and a few co-located instruments (SO2 and CO analyzers, meteorological data) to measure the concentration and chemical composition of NR-PM1 on the top of the Beijing meteorological tower (260 m). This 3-months field campaign was divided into 3 distinct periods: the APEC summit in the middle of the campaign, during which the Chinese Government implemented strict emission control at Beijing and the surrounding regions, a non-heating period before the summit, and a heating period after the summit.

I think that the authors have a very interesting dataset in the hands, and that the measurements performed simultaneously at ground level and at 260 m height can help to better understand the evolution, dispersion, and transport of different kind of particles as a function of meteorological conditions. I would recommend the publication of this manuscript in *Atmospheric Chemistry and Physics* after the authors address the following comments.

We thank the reviewer's positive comments.

Specific comments:

1) Page 4, lines 14-15: Can the authors give some clarifications about the ACSM vs. HR-ToF-AMS inter-comparison they performed during two weeks? Why did they use variable scaling factors for the correction of the ACSM data? Did they also compare PMF analysis between the two instruments? It would be also interesting if the authors mention whether the bias between their two instruments are consistent with those reported by Crenn et al. (2015) and Fröhlich et al. (2015).

Good point. We did a two-week inter-comparison between HR-ToF-AMS and ACSM measurements before this study. The ACSM measurements were further corrected using the regression slopes against HR-ToF-AMS measurements (0.61–1.24) from the inter-comparisons to reduce the uncertainties in vertical comparisons. As shown in Figure R3, all NR-PM_1 species are well correlated between the two instruments (R^2=0.97–1) and the slopes ranged from 0.61–1.24. The different scaling factors for different species mainly due to that the ACSM measurements can have uncertainties of 9–36% for different NR-PM_1 species, consistent with the results reported previously (Crenn et al., 2015). Such information was now added in section 2.2.

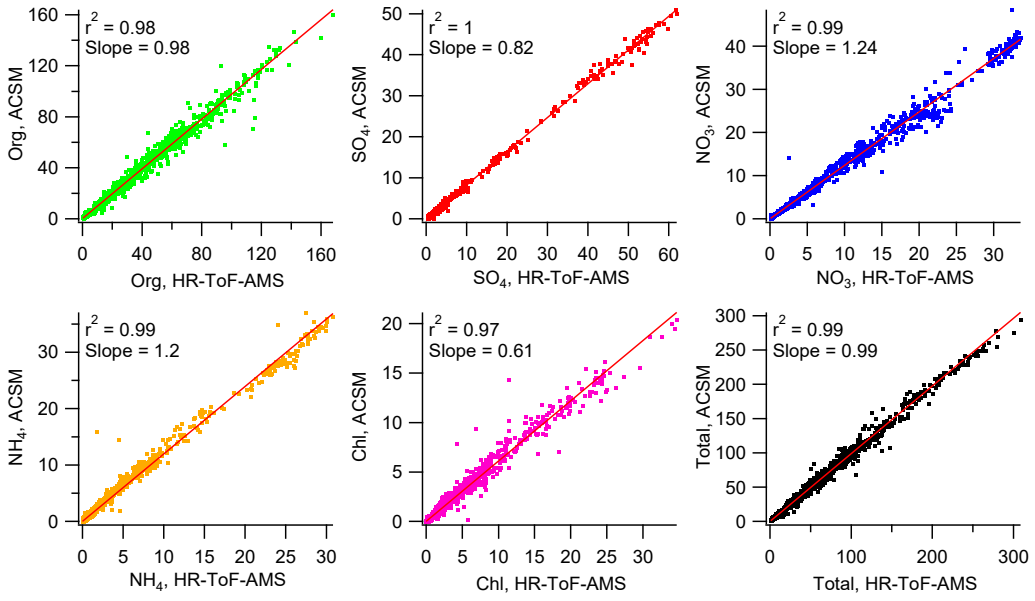

Figure R3. Inter-comparisons between ACSM and HR-ToF-AMS measurements for different NR-PM_1 species.

We also compared the OA factors resolved from PMF analysis of the two datasets during the inter-comparison period. As shown in Figure R4, the mass spectra and time series of three OA factors are overall similar between ACSM and HR-ToF-AMS. However, we also noticed some differences in both mass spectra and time series. In particular, HR-ToF-AMS appears to report higher COA concentrations than ACSM, while the CCOA concentrations are relatively low. Comparatively, the OOA concentrations agree well between the two instruments. Therefore, we used ME-2

analysis to constrain POA factors at 260 m using those resolved at ground site for better comparisons at the two different heights. In addition, the mass spectrum of ACSM OOA presented higher f_{44} than that of HR-ToF-AMS, which is consistent with that reported by Fröhlich et al. (2015), and also explained the high f_{44} in OOA spectrum in this study.

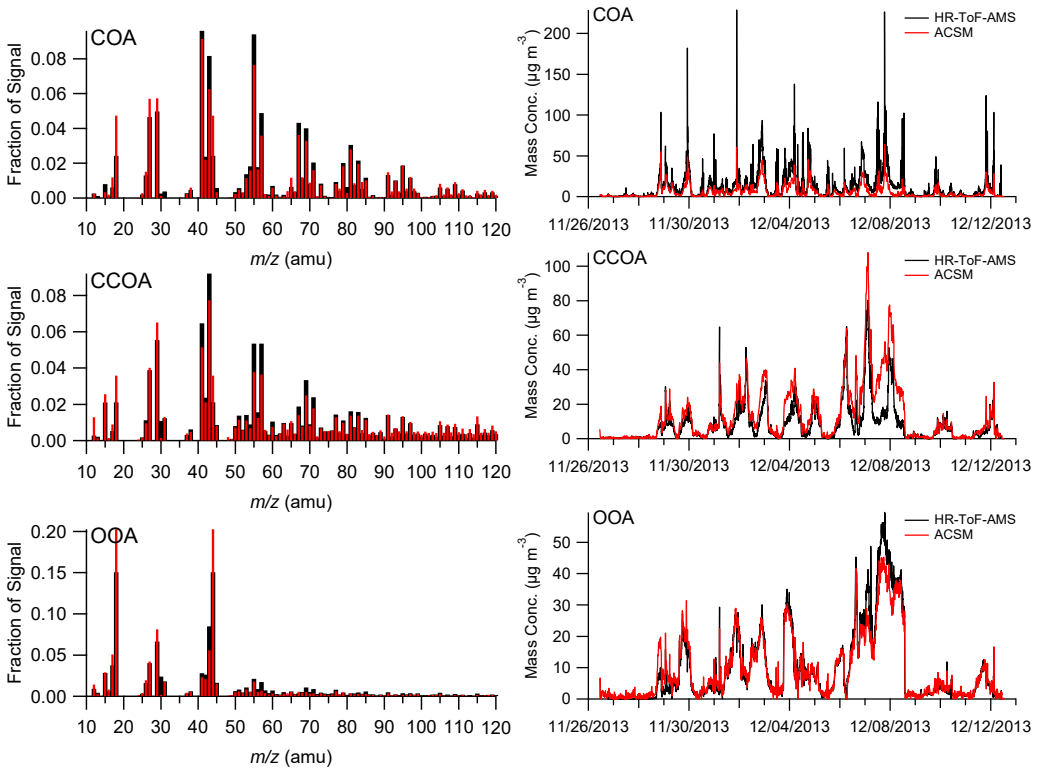

Figure R4. Inter-comparisons of mass spectra and time series of three OA factors from PMF analysis of ACSM and HR-ToF-AMS organic mass spectra. The red and black lines represent ACSM and HR-ToF-AMS solutions, respectively.

2) Page 4, lines 23-24: The FFOA factor is also characterized by a high *m/z* 57/55 ratio. Moreover, given that the PMF analysis has been performed with unit mass resolution data, how do the authors know that signals at high *m/z* correspond to PAH fragments?

Good points. PMF analysis was performed to the unit mass resolution spectra of OA (*m/z* 12−350) that were measured with HR-ToF-AMS, which supplied the information at large *m/z*'s (>150). Figure S1 showed that resolved FFOA spectrum showed strong

PAH signatures, which are *m/z*'s 152, 165, 178, 189, 202, 215, 226, 239… (Dzepina et al., 2007), consistent with the results at the same site (Sun et al., 2016b). Hu et al. (2016) also reported the pronounced peaks of PAHs at *m/z*'s 152, 165, 178 and 189 in the CCOA spectrum in Beijing. Moreover, Sun et al. (2016b) found that CCOA was tightly correlated with PAHs, which was also observed for FFOA in this study (Figure R5). Therefore, we concluded that signals at high *m/z* correspond to PAHs fragments.

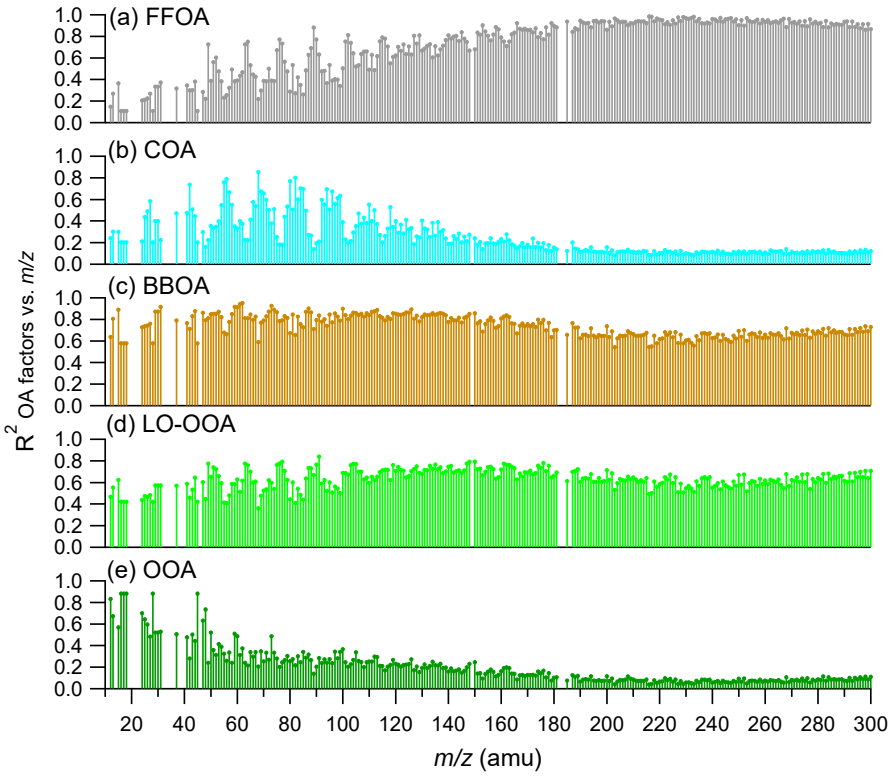

Figure R5. Correlations of five OA factors resolved from the HR-ToF-AMS with each unit *m/z*.

3) Page 8, lines 11-19: The authors mention that the diurnal pattern of FFOA was very pronounced at ground level, and much more flat at 260 m (Figure 7). Is it possible that this result is due to frequent temperature inversions which prevent vertical dispersion of FFOA, exactly like for COA (page 8, lines 28-29)?

Yes, we agree with the reviewer that the more flat FFOA diurnal pattern at 260 m than the ground level could be due to the frequent temperature inversions that

suppressed the vertical mixing of FFOA from local emissions. Following the reviewer's suggestions, we added such an explanation in the revised manuscript, and now it reads:

"One explanation is the frequent temperature inversions at nighttime that suppressed the vertical convection of local FFOA to high heights."

4) Page 9, line 30 to page 10, line 1: I don't think that a high f43/f44 ratio is an argument supporting that LO-OOA corresponds to combustion-related SOA. Indeed, previous studies showed that OOA factors with high f43/f44 ratios can also correspond to factors with biogenic influences (Fig. 4 in Ng et al., 2010; Setyan et al., 2012).

Thanks the reviewer's for pointing this out. We concluded that LO-OOA was a combustion-related SOA mainly because that biogenic emissions are not expected to be important in winter in Beijing.

Technical comments:

5) Page 2, line 20: "from direct~~ion~~ emissions and secondary OA".

Thanks for the reviewer's carefulness. We revised the sentence in the revised manuscript. It now reads:

"…primary OA (POA) from direct emissions and secondary OA (SOA) from …"

6) Section 2.3 (Positive matrix factorization): the authors named the two oxygenated OA factors "OOA" and "LO-OOA". Just to be consistent, I would suggest naming the first factor "MO-OOA" (more oxidized OOA) throughout the manuscript.

Thanks the reviewer's suggestion. Such an OOA factor is typically called as MO-OOA in previous studies. However, our recent study (Sun et al., 2016a) showed that higher f_{44} (fraction of *m/z* 44 in OA) does not necessarily correspond to higher

oxygen-to-carbon (O/C) ratio. Also, this OOA factor was better correlated with nitrate than sulfate in our study, which is generally different from previous findings that MO-OOA was better correlated with sulfate. Therefore, the second SOA factor was named as OOA rather than MO-OOA to avoid confusions.

7) Page 5, line 2: I believe the authors wanted to say "a clear decrease of the ratio**s** of *m/z* 41/43 ~~**to**~~ **and** *m/z* 55/57 as a-value increases".

Yes. We have revised the sentence following the reviewer's suggestions. It now reads:

"…the FFOA spectrum showed a clear decrease of the ratios of *m/z* 41/43 and *m/z* 55/57 as a-value increases …"

8) Page 8, lines 13-14: I would suggest saying "the FFOA concentrations at ground level ~~**dropped**~~ **started to drop** rapidly at ~3:00–4:00".

Thanks for the reviewer's suggestion. We revised the sentence in the new version of the manuscript. It now reads:

"…the FFOA concentrations at ground level started to drop rapidly at ~3:00–4:00"

9) Table 1: The sum of the 5 PMF factors do not match the total organic concentration reported above in the Table. I'm wondering whether the authors should scale the PMF factors to the total organics.

We thank the reviewer's comments. The differences were due to the residuals in ME-2 analysis that cannot be explained by the five OA factors. The unexplained residuals on average account for 4 – 7% of total OA. PMF analysis of HR-ToF-ACSM organic spectra also have similar residuals. To be consistent, we did not scale the sum of OA factors to the total organics in this study.

10) Figure 1: I would suggest using a darker grey to highlight the different periods of interest.

Following the reviewer's suggestions, we changed the color from light grey to dark grey in Figure 1 in the revised manuscript.

11) Figure 4: Is it possible to include the diurnal patterns of the wind direction and CO?

Thanks the reviewer's suggestions. We calculated the diurnal patterns of wind direction and CO and added this figure in supplementary in the revised manuscript.

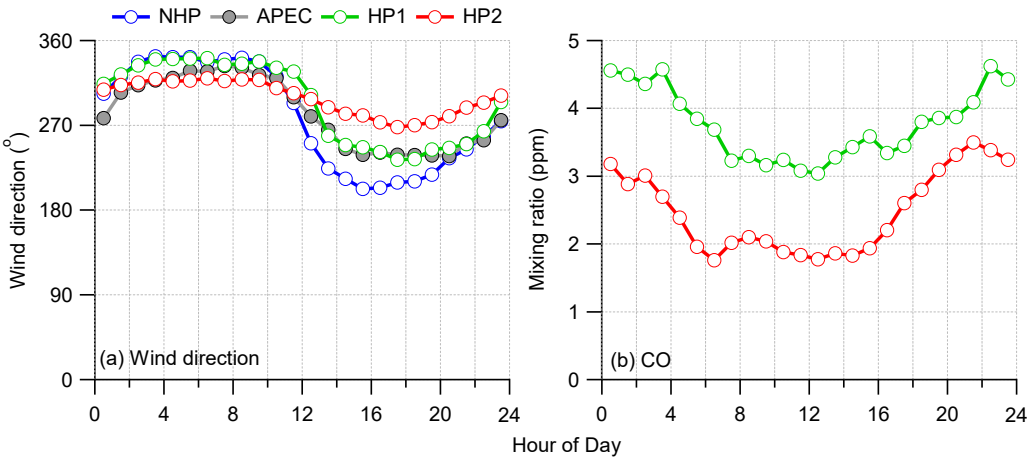

Figure R6. Diurnal variations of (a) wind direction and (b) CO during the four different periods, i.e., NHP, APEC, HP1, HP2. Note that the CO data were not available during NHP and APEC.

12) Figure 5: I'm not sure whether it makes sense to compare the time series of BBOA and LO-OOA with *m/z* 60 and *m/z* 43, respectively. They correspond to the most representative signals of these two factors, and thus cannot be considered as external tracers. For LO-OOA, I would suggest to do the comparison with the time series of Chl, given that they presumably come from the same source (coal combustion).

Thanks for the suggestions. *m/z* 60 and *m/z* 43 are the most representative signals of BBOA and LO-OOA, respectively, rather than the external tracers. We compared the time series of BBOA and LO-OOA with *m/z* 60 and *m/z* 43, respectively, to illustrate the typical mass spectral peaks of these two factors.

We agree with the reviewer that LO-OOA can be correlated with chloride that is mainly from coal combustion in winter in Beijing. Indeed, LO-OOA was well correlated with Chl during HP1 and HP2 (R^2=0.71-0.81). Because this study also covers non-heating season when biomass burning could be a more important source of chloride, we did not show chloride as an external tracer in Figure 5. In fact, the correlations between LO-OOA and Chl were much weaker during NHP and APEC (Figure 6). Still, the comparisons of correlations between LO-OOA and Chl were performed and shown in Figure 6 (right panel).

13) Figure 8: Is there a reason for which the pie charts for 260 m are bigger than those for the ground site? The sizes do not seem to be related to the average concentrations.

Thanks the reviewer's carefulness. Yes, the sizes are not related to the average concentrations which are already shown on the top of pie charts. Because this study is focused on OA characterization at 260 m, we make the pie charts at 260 m bigger than those at ground level to highlight the results.

14) Figure S3: For each time series (right panels), I would suggest to add the average concentration obtained with each a-value, as well as the correlation coefficient (r2) and slope vs. the time series obtained for a-value = 0. With this information, the reader will better see how the time series deviate from the unconstrained factors when the a-value increases from 0.1 to 0.5.

Good points. The average concentrations of five OA factors obtained with each a-value have been presented in Figure S2(c). Following the reviewer's suggestions, we added more visual details on the comparisons between different a-values in the revised manuscript (Table S1). A small point to note is that a-value = 0 means the complete constrained condition rather than the unconstrained mode.

Table S1. The average concentrations for OA factors obtained with each a-value

(Avg). Also shown are the correlation coefficients (R^2) and regression slopes (Slope) when a-value ranges from 0.1-0.5 versus the time series obtained for a-value = 0 for each OA factor.

	a-value=0	**a-value=0.1**	**a-value=0.2**	**a-value=0.3**	**a-value=0.4**	**a-value=0.5**
FFOA	Avg=3.8	Avg=4.0 R^2=0.99 Slope=1.04	Avg=3.6 R^2=0.97 Slope=0.95	Avg=3.7 R^2=0.96 Slope=0.95	Avg=3.7 R^2=0.97 Slope=0.99	Avg=4.3 R^2=0.96 Slope=1.15
COA	Avg=3.1	Avg=3.3 R^2=1.00 Slope=1.04	Avg=3.2 R^2=0.96 Slope=0.93	Avg=3.1 R^2=0.90 Slope=0.81	Avg=2.9 R^2=0.89 Slope=0.76	Avg=2.9 R^2=0.89 Slope=0.77
BBOA	Avg=2.7	Avg=3.2 R^2=0.99 Slope=1.17	Avg=3.7 R^2=0.97 Slope=1.36	Avg=4.1 R^2=0.94 Slope=1.48	Avg=4.5 R^2=0.93 Slope=1.56	Avg=4.6 R^2=0.91 Slope=1.54
LO-OOA	Avg=5.9	Avg=5.5 R^2=1.00 Slope=0.91	Avg=5.3 R^2=0.97 Slope=0.89	Avg=5.2 R^2=0.95 Slope=0.88	Avg=5.2 R^2=0.96 Slope=0.86	Avg=4.9 R^2=0.94 Slope=0.78
OOA	Avg=11.0	Avg=10.7 R^2=1.00 Slope=0.97	Avg=10.8 R^2=1.00 Slope=0.99	Avg=10.5 R^2=1.00 Slope=0.96	Avg=10.2 R^2=1.00 Slope=0.94	Avg=9.8 R^2=1.00 Slope=0.89

Response to Reviewer #3

Comments:

The manuscript by Zhou et al. presents a detailed chemical characterization of organic aerosol at 260 m on a meteorological tower in urban Beijing by using ACSM measurements. Although the real-time measurements of aerosol particle composition at 260 m have been reported previously, this study is unique in terms of the first source apportionment analysis of OA at 260 m by using the multi-linear engine (ME-2) with the constrained POA factors identified at ground site. Fossil fuel-related OA (FFOA) dominantly from coal combustion emissions showed a large increase during heating period (HP). The SOA composition (i.e., LO-OOA and OOA) changed significantly from non-heating period (NHP) to HP. In addition, this study also observed very different OA composition between ground level and 260 m. Bivariate polar plots and back trajectory analysis further illustrated the different source regions of OA factors in different seasons. This manuscript is generally well written and I recommend it for publication after minor revisions.

We thank the reviewer's positive comments.

1.2. FFOA was still a mixture of HOA and CCOA. Did the authors try to extend the PMF solution of HR-AMS to more factors to see if HOA and CCOA can be separated? And also a comparison and discussion with previous AMS-resolved OA factors by the same group in urban Beijing during wintertime will be useful as sometimes HOA and CCOA can be separated but sometimes not.

Yes, it is very challenging to separate the traffic-related HOA from coal combustion OA (CCOA) through PMF analysis of unit mass resolution mass spectra of either HR-ToF-AMS or ACSM. The reasons include: (1) very similar spectral patterns between HOA and CCOA at m/z < 120; (2) very similar temporal variations and diurnal cycles; (3) limited sensitivity of the ACSM, particularly for m/z's > 50 with large uncertainties in ion transmission efficiencies. Sun et al. (2016b) was able to

separate HOA from CCOA by using PMF analysis of high resolution mass spectra and the unit mass resolution mass spectra to *m/z* = 350, while they were not separated in this study even extending the solution to 6 or 7 factors. Therefore, the two sources are combined into one factor, i.e., fossil fuel related OA (FFOA). The FFOA spectrum pattern identified in this study resembles much more to that of smoky coal (Lin et al., 2017) than the standard traffic-related HOA (Ng et al., 2011). Consistent with our previous results in the winter of 2013–2014 (Sun et al., 2016b), FFOA showed dramatic increase after the heating season start on 15 November, and we also found strong PAH signatures in the FFOA spectrum. These results together indicated that FFOA was dominantly from the coal combustion.

3. Please define the polluted and clean episodes in the text.

Good point. The polluted episodes including the formation, evolution and cleaning stages are marked in grey in Figure 1, and the average mass concentrations of NR-PM_1 during polluted episodes are generally larger than 50 μg m^{-3}. The rest periods are defined as clean periods. It is now clarified in the revised manuscript as:

"the changes in NR-PM_1 were characterized by routine cycles of polluted episodes (marked in grey in Fig. 1) and clean periods (the rest of the time) during HP2"

4. Line 20-25 in Page 2, "and also highlight the importance of", change "highlight" to "highlighted".

Thanks for the reviewer's carefulness. We revised the grammatical mistake in the revised manuscript. Now it reads:

"… and also highlighted the importance of OA in the rapid formation of severe haze"

5. Line 5-10 in Page 3, change "as a response of" to "as responses of".

Thanks for pointing this out. Yes, we revised the sentence in the new version of the

manuscript. Now it reads:

"The results showed similar reductions … as responses of emission controls"

6. Line 10 in Page 3, change "was all limited" to "were all limited".

Thanks for the reviewer's carefulness. We revised the singular and plural forms in the manuscript. Now it reads:

"…PMF analyses of OA at 260 m in previous studies were all limited to…"

7. Line 15-20 in Page 4, change "that were measured with HR-AMS" to "that was measured with HR-AMS".

Thanks for the suggestions. Yes, we checked the sentence and found that this is a mistake, which lies in the "as that of ACSM" rather than "that were measured with HR-AMS". We revised it and now it reads:

"…performed to the unit mass resolution spectra of OA (*m/z* 12−350) at ground site that were measured with HR-AMS during the same period as those of ACSM"

8. Line 20-25 in Page 5, change "followed by a short period of clean days" to "followed by short periods of clean days".

We thank the review for pointing this mistake. We revised this and now it reads:

"…followed by short periods of clean days…"

9. Line 25 in Page 6, change "in the major mechanism" to "is the major mechanism".

Yes, we revised the sentence following the reviewer's suggestion. Now it reads:

"… SO_2 by NO_2 in aerosol water is the major mechanism"

References:

Crenn, V., Sciare, J., Croteau, P. L., Verlhac, S., Fröhlich, R., Belis, C. A., Aas, W., Äijälä, M., Alastuey, A., Artiñano, B., Baisnée, D., Bonnaire, N., Bressi, M., Canagaratna, M., Canonaco, F., Carbone, C., Cavalli, F., Coz, E., Cubison, M. J., Esser-Gietl, J. K., Green, D. C., Gros, V., Heikkinen, L., Herrmann, H., Lunder, C., Minguillón, M. C., Močnik, G., O'Dowd, C. D., Ovadnevaite, J., Petit, J. E., Petralia, E., Poulain, L., Priestman, M., Riffault, V., Ripoll, A., Sarda-Estève, R., Slowik, J. G., Setyan, A., Wiedensohler, A., Baltensperger, U., Prévôt, A. S. H., Jayne, J. T., and Favez, O.: ACTRIS ACSM intercomparison – Part 1: Reproducibility of concentration and fragment results from 13 individual Quadrupole Aerosol Chemical Speciation Monitors (Q-ACSM) and consistency with co-located instruments, Atmos. Meas. Tech., 8, 5063-5087, 10.5194/amt-8-5063-2015, 2015.

Dzepina, K., Arey, J., Marr, L. C., Worsnop, D. R., Salcedo, D., Zhang, Q., Onasch, T. B., Molina, L. T., Molina, M. J., and Jimenez, J. L.: Detection of particle-phase polycyclic aromatic hydrocarbons in Mexico City using an aerosol mass spectrometer, Int. J. Mass Spectrom., 263, 152-170, 10.1016/j.ijms.2007.01.010, 2007.

Fröhlich, R., Crenn, V., Setyan, A., Belis, C. A., Canonaco, F., Favez, O., Riffault, V., Slowik, J. G., Aas, W., Aijälä, M., Alastuey, A., Artiñano, B., Bonnaire, N., Bozzetti, C., Bressi, M., Carbone, C., Coz, E., Croteau, P. L., Cubison, M. J., Esser-Gietl, J. K., Green, D. C., Gros, V., Heikkinen, L., Herrmann, H., Jayne, J. T., Lunder, C. R., Minguillón, M. C., Močnik, G., O'Dowd, C. D., Ovadnevaite, J., Petralia, E., Poulain, L., Priestman, M., Ripoll, A., Sarda-Estève, R., Wiedensohler, A., Baltensperger, U., Sciare, J., and Prévôt, A. S. H.: ACTRIS ACSM intercomparison – Part 2: Intercomparison of ME-2 organic source apportionment results from 15 individual, co-located aerosol mass spectrometers, Atmos. Meas. Tech., 8, 2555-2576, 10.5194/amt-8-2555-2015, 2015.

Hu, W., Hu, M., Hu, W., Jimenez, J. L., Yuan, B., Chen, W., Wang, M., Wu, Y., Chen, C., Wang, Z., Peng, J., Zeng, L., and Shao, M.: Chemical composition, sources, and aging process of submicron aerosols in Beijing: Contrast between summer and winter, J. Geophys. Res. - Atmos., 121, 1955-1977, 10.1002/2015jd024020, 2016.

Lin, C., Ceburnis, D., Hellebust, S., Buckley, P., Wenger, J., Canonaco, F., Prévôt, A. S. H., Huang, R.-J., O'Dowd, C., and Ovadnevaite, J.: Characterization of Primary Organic Aerosol from Domestic Wood, Peat, and Coal Burning in Ireland, Environ. Sci. Technol., 51, 10624-10632, 10.1021/acs.est.7b01926, 2017.

Ng, N. L., Canagaratna, M. R., Jimenez, J. L., Zhang, Q., Ulbrich, I. M., and Worsnop, D. R.: Real-Time Methods for Estimating Organic Component Mass Concentrations from Aerosol Mass Spectrometer Data, Environ. Sci. Technol., 45, 910-916, 10.1021/es102951k, 2011.

Sun, Y., Jiang, Q., Wang, Z., Fu, P., Li, J., Yang, T., and Yin, Y.: Investigation of the sources and evolution processes of severe haze pollution in Beijing in January

2013, Journal of Geophysical Research: Atmospheres, 119, 4380-4398, 10.1002/2014JD021641, 2014.

Sun, Y., Du, W., Fu, P., Wang, Q., Li, J., Ge, X., Zhang, Q., Zhu, C., Ren, L., Xu, W., Zhao, J., Han, T., Worsnop, D., and Wang, Z.: Primary and secondary aerosols in Beijing in winter: sources, variations and processes, Atmos. Chem. Phys., 16, 8309-8329, 10.5194/acp-16-8309-2016, 2016a.

Sun, Y., Du, W., Fu, P., Wang, Q., Li, J., Ge, X., Zhang, Q., Zhu, C., Ren, L., Xu, W., Zhao, J., Han, T., Worsnop, D. R., and Wang, Z.: Primary and secondary aerosols in Beijing in winter: sources, variations and processes, Atmos. Chem. Phys., 16, 8309-8329, 10.5194/acp-16-8309-2016, 2016b.

Sun, Y. L., Wang, Z. F., Fu, P. Q., Yang, T., Jiang, Q., Dong, H. B., Li, J., and Jia, J. J.: Aerosol composition, sources and processes during wintertime in Beijing, China, Atmos. Chem. Phys., 13, 4577-4592, 10.5194/acp-13-4577-2013, 2013.

Zhang, J. K., Cheng, M. T., Ji, D. S., Liu, Z. R., Hu, B., Sun, Y., and Wang, Y. S.: Characterization of submicron particles during biomass burning and coal combustion periods in Beijing, China, Sci. Total. Environ., 562, 812-821, 10.1016/j.scitotenv.2016.04.015, 2016.

Characterization and source apportionment of organic aerosol at 260 m on a meteorological tower in Beijing, China

Wei Zhou[1,2], Qingqing Wang[1], Xiujuan Zhao[3], Weiqi Xu[1,2], Chen Chen[1], Wei Du[1,2], Jian Zhao[1,2], Francesco Canonaco[4], André S. H. Prévôt[4], Pingqing Fu[1,2], Zifa Wang[1,2], Douglas R. Worsnop[5] and Yele Sun[1,2,6]

[1]State Key Laboratory of Atmospheric Boundary Layer Physics and Atmospheric Chemistry, Institute of Atmospheric Physics, Chinese Academy of Sciences, Beijing 100029, China

[2]University of Chinese Academy of Sciences, Beijing 100049, China

[3]Institute of Urban Meteorology, China Meteorological Administration, Beijing 100089, China

[4]Laboratory of Atmospheric Chemistry, Paul Scherrer Institute, Villigen PSI 5232, Switzerland

[5]Aerodyne Research, Inc., Billerica, MA, USA

[6]Center for Excellence in Regional Atmospheric Environment, Institute of Urban Environment, Chinese Academy of Sciences, Xiamen 361021, China

Correspondence to: Yele Sun (sunyele@mail.iap.ac.cn)

Abstract. Despite extensive efforts into characterization of submicron aerosols at ground level in the megacity of Beijing, our understanding of aerosol sources and processes at high altitudes remains less understood. Here we conducted a three-month real-time measurement of non-refractory submicron aerosol (NR-PM_1) species at a height of 260 m from 10 October 2014 to 18 January 2015 using an aerosol chemical speciation monitor. Our results showed a significant change in aerosol composition from non-heating period (NHP) to heating season (HP). Organics and chloride showed clear increases during HP due to coal combustion emissions, while nitrate showed substantial decreases from 28% to 15–18%. We also found that NR-PM_1 species in heating season can have average mass differences of 30–44% under similar emission sources yet different meteorological conditions. Multi-linear engine 2 (ME-2) using three primary organic aerosol (OA) factors, i.e., fossil fuel-related OA (FFOA) dominantly from coal combustion emissions, cooking OA (COA), biomass burning OA (BBOA) resolved from ground high-resolution aerosol mass spectrometer measurements as constrains was performed to OA mass spectra of ACSM. Two types of secondary OA (SOA) that were well correlated with nitrate and chloride/CO, respectively, were identified. SOA played a dominant role in OA during all periods at 260 m although the contributions were decreased from 72% during NHP to 58–64% during HP. The SOA composition also changed significantly from NHP to HP. While the contribution of oxygenated OA (OOA) was decreased from 56–63% to 32–40%, less oxidized OOA (LO-OOA) showed a large increase from 9–16% to 24–26%. COA contributed a considerable fraction of OA at high altitude, and the contribution was relatively similar across different periods (10–13%). In contrast, FFOA showed a large increase during HP due to the influences of coal combustion emissions. We also observed very different OA composition between ground level and 260 m. Particularly, the contributions of COA and BBOA at ground site were nearly twice those at 260 m, while SOA at

260 m was ~15–34% higher than that at ground level. Bivariate polar plots and back trajectory analysis further illustrated the different source regions of OA factors in different seasons.

~~0~~1 Introduction

Atmospheric aerosol particles reduce visibility by scattering and absorbing solar radiation, and also exert detrimental effects on human health (Dockery et al., 1993; IPCC, 2013). Beijing, the capital of China, has been suffering severe haze pollution since the last decade, especially in autumn and winter (Huang et al., 2014; Guo et al., 2014). For example, Beijing released the first air pollution red alert due to a severe haze episode in December 2015 when the daily $PM_{2.5}$ concentration exceeded 300 μg m^{-3} for more than 3 days. Therefore, the sources and formation mechanisms of haze episodes have been extensively investigated for mitigating air pollution in Beijing in recent years (Zhao et al., 2013b; Huang et al., 2014; Yang et al., 2015; Sun et al., 2016a; ~~Zhao et al., 2013b; Yang et al., 2015;~~ Wu et al., 2017). The results highlight that stagnant meteorological conditions with shallow planetary boundary layer (PBL) and low surface wind, traffic and coal combustion emissions, regional transport and secondary productions of SNA (sulfate, nitrate, and ammonium) are the major factors leading to the formation of severe haze episodes. However, our knowledge of the characteristics of aerosol particles is far from complete, mainly due to the fact that most previous studies were conducted at ground sites and were subject to strong influences from local emissions. The measurements and analysis at high ~~altitudes in~~heights at urban sites are still very limited, particularly long-term analysis by covering different seasons.

Organic aerosol (OA) accounts for a major mass fraction (20–90%) of submicron aerosol (Zhang et al., 2007), and comprises primary OA (POA) from ~~direction~~direct emissions and secondary OA (SOA) from oxidation of volatile organic compounds (VOCs) (Jimenez et al., 2009). The deployments of Aerodyne Aerosol Mass Spectrometer (AMS)/Aerosol Chemical Speciation Monitor (ACSM) for real-time measurements of aerosol particle composition followed by subsequent positive matrix factorization (PMF) analysis (Paatero and Tapper, 1994; Ulbrich et al., 2009) have greatly improved our understanding on the sources of OA in China, and also ~~highlight~~highlighted the important role of OA in the rapid formation of severe haze (Huang et al., 2014; Sun et al., 2014; Zhang et al., 2014). The sources and formation of OA are seasonally different. For example, SOA is more significant than POA in summer due to stronger photochemical processing, while POA often plays a more important role than SOA in winter due to more primary emissions, e.g., coal combustion, and weaker photochemistry (Sun et al., 2015b; Li et al., 2017; Ma et al., 2017). A recent study by Xu et al. (2017) further found that photochemical processing tends to form less oxidized SOA (LO-OOA), while aqueous-phase processing can form more oxidized SOA (MO-OOA).

Despite extensive OA studies in recent years, our understanding of the sources and processes of OA at ~~a~~ high ~~altitude~~heights in megacities is still limited. Sun et al. (2015a) conducted the first real-time measurements of aerosol particle composition at 260 m on the Beijing 325 m meteorological tower (BMT) using an ACSM. A high-resolution time-of-flight AMS (HR-AMS hereafter) was deployed in parallel at ground level during the same period. The results showed substantially

different aerosol composition between 260 m and ground level, particularly, OA showed higher contribution to non-refractory PM_1 (NR-PM_1) at ground level (65%) than 260 m (54%). Source apportionment of OA further illustrated the similar temporal variations of SOA at the two heights, while those of POA were dramatically different. Also, the contribution of SOA to OA at higher altitude was higher than that at ground site (49% vs. 38%). Chen et al. (2015) further analyzed OA at 260 m before and during Asia-Pacific Economic Cooperation (APEC) summit when strict emission controls were implemented in Beijing and surrounding regions. The results showed similar reductions in POA and SOA at 260 m during APEC as ~~a response~~responses of emission controls. However, POA remained at small changes at ground level although SOA showed similar reductions as that at 260 m~~. Such differences highlight the different impacts of local source emissions and regional transport on POA and SOA at different altitudes in the city. Note that PMF analysis of OA at 260 m in previous studies was all limited to a 2-factor solution, i.e.,~~ (Xu et al., 2015). Such differences highlight the different impacts of local source emissions and regional transport on POA and SOA at different heights in the city. Note that PMF analyses of OA at 260 m in previous studies were all limited to a two-factor solution, i.e., POA and SOA. Although the mass spectrum of POA shows a mix of different primary emissions, e.g., traffic, cooking and biomass burning, the solutions with more factors however showed unrealistic split of OA factors (Sun et al., 2015a; Chen et al., 2015). As a consequence, the variations and evolution of different POA and SOA factors are poorly understood at a high altitude in Beijing. For example, Zhao et al. (2017) found that the two different SOA factors, i.e., LO-OOA and MO-OOA showed different responses to emission controls during the 2015 China Victory Day parade at ground site. While MO-OOA showed a large decrease during the control period, LO-OOA was comparable during and after the control period. However, the composition and variations of different SOA factors at 260 m were never characterized. This also greatly limits our understanding of the sources and processes of OA at high ~~altitudes~~heights in the ~~planetary~~low atmospheric boundary layer in Beijing.

In this study, an ACSM was deployed at 260 m on the BMT for three months to measure NR-PM_1 aerosol species in real-time. This study encompasses three periods with different emission scenarios, i.e., non-heating period (NHP), APEC with strict emission controls in Beijing and surrounding regions, and heating period (HP) with significant influences from coal combustion emissions. The characteristics and sources of NR-PM_1 and OA before and during APEC were ~~characterized~~reported in our previous study (Chen et al., 2015), here we mainly focus on characterization of submicron aerosols during the heating season, and also the comparisons with those during NHP and APEC. Most importantly, we present the first source apportionment analysis of OA at 260 m by using the multi-linear engine (ME-2) with the constrained POA factors identified at ground site. The mass concentrations, composition, and diurnal cycles of POA and SOA factors are characterized, and the changes in POA and SOA composition from NHP to APEC and HP are elucidated. Also, the comparisons of sources and composition of POA and SOA between ground level and 260 m are presented.

2 Experimental methods

2.1 Sampling site and measurements

The NR-PM_1 species, including organics (Org), sulfate (SO_4), nitrate (NO_3), ammonium (NH_4), and chloride (Chl), and gaseous species of SO_2 and CO, were measured at the height of 260 m on the BMT (39°58′28″N, 116°22′16″E, ASL: 49 m) using an ACSM and gas analyzers (Thermo Scientific). A more detailed description of the sampling site and the operations of the ACSM can be found in Sun et al. (2015a) and Chen et al. (2015). Simultaneously, a HR-AMS was deployed at the ground level to measure the size-resolved NR-PM_1 composition (Xu et al., 2015). In addition, the meteorological variables including wind direction (WD), wind speed (WS), relative humidity (RH), and temperature (*T*) were measured at 8 m and 280 m ~~were also measured~~ on the BMT.

2.2 ACSM data analysis

The mass concentrations and chemical compositions of NR-PM_1 were analyzed with the ACSM standard data software (V1.5.3.0). Consistent with our previous study in Beijing in 2014 (Chen et al., 2015), we used the same parameters for the entire campaign. For example, a constant collection efficiency (CE) of 0.5 was applied to compensate for the incomplete detection of aerosol particles which is primarily caused by particle bounce effects at the vaporizer (Matthew et al., 2008). The reason is that the mass fraction of ammonium nitrate, RH and particle acidity were found to play minor influences on CE in this study (Middlebrook et al., 2012). ~~Note the ACSM NR-PM_1 species were further corrected using the corresponding scaling factors (0.61–1.24) that were determined from the two-week inter-comparisons between ACSM and HR-AMS.~~A two-week inter-comparison between HR- AMS and ACSM measurements was performed before this study (Sun et al., 2015a). Using the same CE of 0.5, all NR-PM_1 species are well correlated between the measurements from the two instruments (R^2=0.97–1) and the slopes range from 0.61–1.24. To reduce the uncertainties in vertical comparisons, the ACSM measurements were further corrected using the regression slopes against HR-AMS measurements. The different scaling factors for different species were likely due to the fact that the ACSM measurements can have uncertainties of 9–36% for different NR-PM_1 species (Crenn et al., 2015).

2.3 ~~–~~Positive matrix factorization

Positive matrix factorization (PMF) was first performed to the unit mass resolution spectra of OA (*m/z* 12–350) at ground site that were measured with HR-AMS during the same period as ~~that~~those of ACSM. Five factors, i.e., a fossil fuel-related OA (FFOA) from traffic and coal combustion emissions, a cooking-related OA (COA), a biomass burning OA (BBOA), an oxygenated OA (OOA), and a less oxidized OOA (LO-OOA) were determined. Extending the PMF solution to 6 and 7 factors still cannot separate the traffic-related hydrocarbon-like OA (HOA) from coal combustion OA (CCOA). The mass spectra of five OA factors are presented in Fig. S1. Each factor was characterized by the typical prominent peaks indicative

of different sources and properties (Sun et al., 2016b), for example, high *m/z* 60 and 73 peaks in BBOA, prominent PAHs fragments in FFOA, high *m/z* 55/57 in COA, and pronounced *m/z* 44 in SOA (LO-OOA and OOA). The mass spectral profiles of the three POA factors, i.e., FFOA, COA, and BBOA were then used as the constrains of multi-linear engine 2 (ME-2) analysis at 260 m. Compared with the PMF2 algorithm, ME-2 reduces rotational ambiguity by adding the known source information (e.g., factor profiles or factor time series) into the model (~~Canonaco et al., 2013;~~ Paatero and Tapper, 1994; Canonaco et al., 2013). Considering that the POA factors at 260 m might not be completely the same as those at ground site, the so-called a-value approach with a-value ranging from 0 to 0.5 for all three POA factors were ~~performed to OA.~~used in this study. Following the guidelines of the a-value sensitivity test presented by Crippa et al. (2014), we evaluated the mass spectral profiles, diurnal patterns, time series of OA factors, and also compared with external tracers. As shown in Fig. ~~S3~~S2, the time series of FFOA and COA were fairly robust across different a-values, and the differences were generally less than 10%. Although the COA spectrum was also robust, the FFOA spectrum showed a clear decrease of the ~~ratio~~ratios of *m/z* 41/43 ~~to~~and *m/z* 55/57 as a-value increases, and became more different from that of burning smoky coal (Lin et al., 2017). Compared with FFOA and COA, BBOA showed more variability in both spectrum and time series. As a-value increased from 0 to 0.5, the average BBOA concentration was increased by nearly a factor of 2, and the mass spectrum showed a significant decrease of *m/z* 60. To better compare with the PMF results at ground site and also allow for some degrees of freedom for model runs, the five-factor solution with a-value of 0 for FFOA and BBOA and 0.2 for COA was selected in this study. We also performed PMF analysis on ACSM OA spectra, and found that the BBOA factor cannot be resolved although biomass burning is a common source in winter. Figure S4 shows ~~a~~ diurnal ~~comparison~~comparisons of the solutions between PMF and ME-2. It is clear that the unconstrained PMF reports twice higher FFOA and COA than ME-2, while OOA is 30% lower (Fig. S2). While the rotational ambiguity is one of the reasons, another explanation is that FFOA and COA are mixed with BBOA which cannot be ~~resolved~~separated by PMF. More detailed ME-2 diagnostics are presented in Figs. S2–S4.

3 Results and discussion

3.1 Characteristics of NR-PM_1 species at 260 m

3.1.1 Mass concentrations and chemical composition

Figure 1 shows the time series of meteorological parameters and NR-PM_1 species for the entire study, which can be classified into three different periods, i.e., NHP, APEC and HP according to the changes in source emissions. The HP was further separated into two different periods according to the variations in *T* and RH. As shown in Fig. 1, the first HP period (HP1) from 13 November to 31 November showed clearly higher RH and *T* compared with the second period (HP2) from 1

December to 18 January. The NR-PM_1 mass concentration varied significantly throughout the entire study with hourly average concentration ranging from 0.7 to 284.8 μg m^{-3}. Such dramatic variations primarily driven by meteorological changes at ground sites have also been observed many times in autumn and winter in Beijing (Sun et al., 2013b; Guo et al., 2014; Zhang et al., 2016b). For example, the changes in NR-PM_1 were characterized by routine cycles of ~~clean periods and~~ polluted episodes (marked in grey in Fig. 1) and clean periods (the rest of the time) during HP2. Comparatively, polluted episodes that lasted approximately four days and then followed by ~~a~~ short ~~period~~periods of clean days were more frequent during NHP, mainly due to the fewer occurrences of northwesterly winds (Fig. S5). Consistently, periods with high NR-PM_1 loading (> 80 μg m^{-3}) accounted for more time during NHP (37%) than HP2 (25%). Indeed, the average NR-PM_1 concentration during HP2 (48.6 μg m^{-3}) was even lower than that during NHP (64.9 μg m^{-3}), illustrating that the PM pollution in autumn 2014 was more severe than that in winter. The large reduction of NR-PM_1 by 61% during APEC compared with that during NHP due to regional emission controls and favorable meteorological conditions has been reported in Chen et al. (2015) and Sun et al. (2016c). This is also consistent with the fact that the periods with NR-PM_1 less than 60 μg m^{-3} accounted for 93% of the time during APEC, which is much higher than that before APEC (51%).

The two heating periods showed very different PM levels with the average NR-PM_1 concentrations being 74.5 and 48.6 μg m^{-3}, respectively. As shown in Fig. 2, the frequency of NR-PM_1 mass during HP1 was significantly different from that during HP2. Clean periods with NR-PM_1 < 20 μg m^{-3} accounted for nearly half of the total time during HP2, while it was much less during HP1 (34%). Considering that emission sources could not have significant changes during the heating season, such differences were mainly caused by the different meteorological conditions, for example more frequent north-westerly winds during HP2 than HP1 (Fig. S5). In addition, the different RH and *T* also indicate the different chemical processing, e.g., photochemical and aqueous-phase processing between HP1 and HP2. Note that the average NR-PM_1 during HP1 was only 15% higher than that during NHP, and that of HP2 was even 25% lower, which appears to contradict with our previous conclusion that HP showed approximately 50% higher PM loading than NHP (Wang et al., 2015). One major reason is due to more frequent clean periods during HP in 2014 than 2012 (Wang et al., 2015).

Organics comprised the major fraction of NR-PM_1 during all periods, on average accounting for 46–54%. The dominance of organics in NR-PM_1 was consistent with previous studies at ground sites in Beijing (Sun et al., 2013a; Huang et al., 2014; Zhang et al., 2016a). Note that the contribution of organics showed an ~~increased~~increase during HP as a result of enhanced emissions from coal combustion (Wang et al., 2015; Elser et al., 2016; ~~Wang et al., 2015;~~ Zhang et al., 2016b). Consistently, the combustion-related chloride was increased by a factor of ~2 from 4% during NHP to 7–8% during HP, and the mixing ratio of SO_2 was increased from 8.0 to 12.6–13.9 ppb. Our results highlight the great impact of coal combustion on aerosol chemistry at a high ~~altitude~~height in the city. The two secondary inorganic species of sulfate and nitrate showed different variations between NHP and HP. The sulfate contribution during HP (14–15%) remained at similar levels as that during NHP (14%), and the concentrations were also relatively close (6.9–11.2 μg m^{-3} vs. 8.8 μg m^{-3}), while the nitrate

contributions and mass concentrations decreased substantially from NHP (28% and 17.9 μg m^{-3}) to HP (15–18% and 7.4–13.3 μg m^{-3}).

Such differences demonstrate the different formation mechanisms of nitrate and sulfate in different seasons. Nitrate appears to be mainly driven by the photochemical production in wintertime while sulfate is mainly from aqueous-phase/heterogeneous reactions (Sun et al., 2013a). The recent study further ~~highlight~~highlights that the oxidation of SO_2 by NO_2 in aerosol water ~~in~~is the major mechanism (Cheng et al., 2016). As shown in Fig. 3, the SO_4/NO_3 ratios increased similarly along with RH during all periods, indicating that aerosol liquid water exerted a larger impact on the formation of sulfate than nitrate. The large increases in sulfate and SOR (sulfur oxidation ratio) during periods with high RH, for example, SOR was increased from 0.09 (RH = ~45%) to 0.48 (RH = ~85%) during HP1, further supporting the aqueous-phase production of sulfate (Ohta and Okita, 1990). The SO_4/NO_3 ratios were ubiquitously lower than 1 during NHP and APEC, suggesting a more important role of nitrate in PM pollution in autumn. Comparatively, sulfate gradually exceeded nitrate as RH ~~was~~ increased to > 60% during HP, and became the dominant secondary inorganic species. Also note that the SO_4/NO_3 ratios showed large variations (~0.2–10) during periods with low sulfate mass loading (< 3 μg m^{-3}), indicating more source variability during clean periods.

3.1.2 Diurnal variations of NR-PM_1 species

The diurnal variations of meteorological variables, NR-PM_1 species and SO_2 are presented in Fig. 4. A detailed comparison of the diurnal patterns between NHP and APEC was presented in Chen et al. (2015). As shown in Fig. 4, the diurnal patterns of meteorological parameters (RH and WS) were relatively similar between NHP and HP1 except lower *T* during HP1. However, the diurnal patterns of organics, sulfate, and chloride showed ubiquitously higher concentrations during HP1 than NHP throughout the day, supporting the significant influences of coal combustion emissions on these three species (Wang et al., 2015). Two clear organic peaks occurring at lunch and dinner time were observed during both periods, highlighting the influences of cooking emissions at high ~~altitude~~heights in urban Beijing. Note that the differences of organics at nighttime (~30–50%) were larger than those (< 30%) during daytime, consistent with the enhanced coal combustion emissions at nighttime. We also noticed that all NR-PM_1 species during HP1 showed similar diurnal behaviors that were characterized by first gradual decreases from mid-night to early morning (~8:00 ~~am~~), and then increases during the rest of the day. We found that such diurnal patterns were strongly associated with the daily changes in wind direction. For example, the winds were dominantly from the north at nighttime, while they switched to the south/southwest after 12:00~~.~~ (Fig. S6). The increases between 8:00–12:00 can be explained by the corresponding decreases in wind speed (Fig. 4).

The diurnal patterns of NR-PM_1 species during HP2 were similar to those during HP1, yet the mass concentrations were much lower. For example, nitrate showed the largest decrease by 34–55% followed by sulfate (27–48%) and organics (13–50%) during HP2. Considering the similar emission sources between HP1 and HP2, such decreases can be explained by

more frequent north-westerly winds that were associated with higher wind speed and lower RH during HP2 (Fig. 4). This is further supported by the fact that the polluted episodes showed much smaller differences between HP1 and HP2 (e.g., ~20% for NR-PM_1, discussed in Sec.3.3). In addition, the reduced photochemical processing as indicated by the decrease in nitrate during HP2 also played a role. We also note that SO_2 at nighttime during HP2 was even higher than that during HP1, suggesting less transformation of SO_2 into sulfate due to drier conditions (RH = ~30%). Our results demonstrate that meteorological condition is a critical factor affecting the PM levels during heating season in addition to coal combustion emissions. For example, the favorable meteorological condition can cause an average decrease of NR-PM_1 by 35%, varying from 26 to 44% for different aerosol species (Table 1). Therefore, it is critically important to exclude the meteorological effects for an accurate evaluation of the impacts of source emission changes on air quality.

3.2 OA composition, sources and variations

3.2.1 Fossil fuel-related organic aerosol (FFOA)

The FFOA spectrum shows prominent hydrocarbon ion series $C_nH_{2n-1}^+$ (*m/z* 27, 41, 55) and $C_nH_{2n+1}^+$ (*m/z* 29, 43, 57~~) and $C_nH_{2n-1}^+$ (*m/z* 27, 41, 55~~), yet the spectral pattern resembles much more to that of burning of smoky coal (Lin et al., 2017) than the standard traffic-related HOA (R^2 = 0.79) (Ng et al., 2011). These results suggest that FFOA at 260 m is likely dominantly from coal combustion emissions rather than traffic emissions, consistent with the better correlations between FFOA and chloride and SO_2 during HP than NHP (Fig. 6). FFOA was also tightly correlated with CO, a tracer for combustion emissions, during HP (R^2 = 0.62–0.68). As shown in Fig. 5a, the temporal variation of FFOA showed a dramatic increase after the heating season starts on 15 November. The average concentration of FFOA during HP1 and HP2 was 4.7 and 5.2 μg m^{-3}, respectively, which is ~~more than~~nearly 3 times higher than those during NHP and APEC (1.2–1.4 μg m^{-3}), indicating the largely enhanced coal combustion emissions during the heating season. Correspondingly, the FFOA contributions ~~in~~to OA also showed large increases from 5% during NHP to 13–21% during HP. FFOA showed a pronounced diurnal cycle during HP1 and HP2 with nearly twice higher concentration at nighttime than daytime. However, the diurnal pattern was less significant during NHP, indicating the dominant source of regional transport for FFOA at 260 m. The bivariate polar plot of FFOA (Fig. 9a) further indicates that high concentration of FFOA during NHP was dominantly from the regional transport in the southwest. Consistently, the FFOA concentration at 260 m was much higher than that at ground level throughout the day (average: 0.4 μg m^{-3}) during NHP when coal combustion emissions were not important inside the fifth ring road of the city. The diurnal patterns of FFOA were substantially different between ground level and 260 m during HP. Particularly, the diurnal cycles at ground level showed much larger day and night differences. As shown in Figs. 7c and 7d, the FFOA concentrations at ground level ~~dropped~~started to drop rapidly at ~3:00–4:00 and reached the minimum at ~14:00. One explanation is the largely enhanced coal combustion emissions at nighttime for residential heating in local areas. In comparison, the diurnal cycles of FFOA at 260 m were much smoother mainly, and the concentrations in the daytime

were even higher than those at ground level. One explanation is the frequent temperature inversions at nighttime that suppressed the vertical convection of local FFOA to high heights. We also noticed slightly higher FFOA concentration during HP2 (5.2 μg m^{-3}) than HP1 (4.7 μg m^{-3}). The bivariate polar plots in Fig. 9a showed a high FFOA concentration (> 12 μg m^{-3}) region in the southwest during HP2, while it was negligible during HP1 but primarily from the local area. Such a difference in source regions explained the higher FFOA concentration during HP2 than HP1.

3.2.2 Cooking organic aerosol (COA)

COA that contributes a large fraction of OA at ground level in megacities has been widely characterized (~~Crippa~~Allan et al., ~~2013~~ 2010; Sun et al., 2011; Mohr et al., 2012; ~~Allan~~Crippa et al., ~~2010~~2013). However, the characteristics of COA at high ~~altitudes~~heights in megacities were poorly characterized. Our results showed similar diurnal cycles of COA at 260 m to those observed in Beijing and other urban sites (Huang et al., 2010; Sun et al., 2012; Xu et al., 2014~~; Huang et al., 2010~~), which were characterized by two pronounced peaks at meal ~~time~~times. The noon COA peak at 260 m was relatively comparable to that at ground level, mainly due to the vertical mixing associated with the rising boundary layer during daytime. In fact, the COA concentrations were almost the same between ground level and 260 m in the late afternoon (~16:00). In contrast, the night COA peak at 260 m was significantly lower than that at ground level. One explanation is the shallow boundary layer and frequent temperature inversions at night suppressed the vertical mixing of COA to a high altitude. Figure 9b shows that high concentration of COA was mainly located in a small region near the sampling site during all periods, highlighting the dominant local sources of COA. Indeed, the COA mass concentrations were relatively comparable (2.7–4.8 μg m^{-3}) across different periods except APEC (1.2 μg m^{-3}) with strict emission controls (Fig. 5). This is consistent with the fact that cooking emissions are relatively stable during all seasons. The average contributions of COA were also close during four periods, ranging from 10–13%, yet ubiquitously lower than those (18–38%) observed at ground site (Xu et al., 2015). Previous studies have shown that the impact of COA is spatially limited as the concentration decreased rapidly outside of the city (Ots et al., 2016). Our results illustrated the influences of cooking emissions on OA at high ~~altitudes~~heights in megacities, and the impacts are expected to be vertically limited as the concentration decreased with the increasing height.

3.2.3 Biomass burning OA (BBOA)

The average concentrations of BBOA were comparable between NHP (3.0 μg m^{-3}) and HP (2.7–3.2 μg m^{-3}) suggesting that biomass burning was an important source of OA at 260 m in both autumn and winter. Indeed, BBOA accounted for a considerable fraction, 11% and 9–11% during NHP and HP, respectively, of total OA. The BBOA concentration at 260 m was decreased by ~70% during APEC, which is much higher than that (16%) at ground site (Xu et al., 2015). One explanation is that BBOA during APEC was more from regional transport at 260 m (Fig. 9c) while there were still considerable local biomass burning emissions near the sampling site. Note that BBOA was better correlated with secondary

inorganic species during NHP and HP (R^2 = 0.54–0.80) than chloride (Fig. 6), suggesting that BBOA at 260 m was likely relatively well mixed with secondary species over a regional scale. This is also consistent with their similar diurnal patterns (Fig. 4). Although the contributions of BBOA to OA were comparable (7–11%) during the four periods, the sources can be very different. For example, BBOA was mainly from the southwest and southeast of Beijing during NHP, while the concentrations were low in the nearby regions (Fig. 9c). These results suggest that regional transport was the major source of BBOA at 260 m during NHP. Comparatively, BBOA during APEC and HP2 were from both local emissions and the transport from the southwest while it was primarily from local source emissions during HP1. The diurnal variations of BBOA at ground level also showed much higher concentrations at nighttime than daytime during all periods, supporting the strong local biomass burning sources. Indeed, BBOA at ground level accounted for 20–28% of OA during HP, which is more than twice that of at 260 m (9–11%).

3.2.4 Secondary organic aerosol (OOA and LO-OOA)

The mass spectra of two SOA (LO-OOA and OOA) factors were both characterized by the prominent peak of *m/z* 44 (mainly CO_2^+) (Aiken et al., 2009). OOA showed much higher *f*44 than LO-OOA (0.28 and 0.09, respectively), indicating that OOA was more oxidized than LO-OOA (Aiken et al., 2008). Note that LO-OOA was highly correlated with large *m/z*'s (Fig. 6) which appears different from previous findings that POA typically correlates better with high *m/z*'s (Sun et al., 2016b). We noticed that LO-OOA showed much better correlations with external trace species during HP than NHP and APEC. Particularly, LO-OOA was well correlated with chloride (R^2 = 0.71–0.81) and CO (R^2 = 0.79–0.84) that were dominantly from coal combustion emissions in heating season. In addition, the mass spectrum of LO-OOA presented a much higher f_{43}/f_{44} (f_{43}, fraction of *m/z* 43) ratio than previous studies (Wang et al., 2016). All these facts suggest that LO-OOA here was very likely a combustion-related SOA. Consistently, the LO-OOA mass ~~concentration~~concentrations showed ~~a~~ large ~~enhancement~~enhancements from 4.6 and 1.1 μg m^{-3} during NHP and APEC to 8.5 and 6.6 μg m^{-3} during HP1 and HP2, respectively, supporting more fresh SOA production due to enhanced combustion emissions. We also note that the LO-OOA at 260 m was nearly twice that of ground site during NHP and HP1, while they were comparable during HP2. These results might indicate that the polluted conditions with high RH are subject to form more LO-OOA at high altitudes.

OOA dominated OA during both NHP and APEC, accounting for 56% and 63%, respectively. In contrast, the contribution of OOA was largely reduced during HP, accounting for 32–40% of OA. This result indicates a large reduction in production of more oxidized SOA in heating season. As shown in Fig. 6, OOA was highly correlated with nitrate during all four different periods (R^2 = 0.70–0.90), indicating that OOA is likely dominantly from photochemical production as that of nitrate (Sun et al., 2013b). Figure 7 shows that OOA increased significantly in the afternoon due to photochemical processing while that of LO-OOA was less significant. We noticed that OOA was correlated with sulfate during NHP and APEC (R^2 = 0.73 and 0.67), and also periods with high RH during HP1 and HP2 (Fig. ~~S6~~S7). These results together indicate

that OOA likely contains two different types of SOA associated with photochemical and aqueous-phase processing, respectively, yet it is difficult to separate an aqueous-phase SOA factor as that of HR-AMS due to the limited sensitivity of the ACSM and limited specificity of the mass spectra (Sun et al., 2016b).

Overall, OA composition at 260 m varied substantially during the four periods. SOA dominated OA during all periods although the contributions were decreased from 72% during NHP to 58–64% during HP. The SOA composition also changed significantly, particularly LO-OOA showed large increases from 9–16% during NHP to 24–26% during HP. Correspondingly, the OOA contribution was decreased from 56–63% to 32–40%. Compared to the ground site, OA showed 15–34% higher SOA contribution at 260 m, highlighting the importance of SOA at high altitudes in urban areas. In contrast, POA (= FFOA + COA + BBOA) played a more important role in PM pollution at ground during HP by accounting for 57–65%. Particularly, the contributions of COA and BBOA at ground site were nearly twice those of at 260 m. The large differences in OA composition between ground level and 260 m have significant implications that measurements at high ~~altitudes~~heights are of great importance for validating and improving the model simulations of POA and SOA in ~~the~~ future studies.

3.3 Comparisons between clean and polluted episodes

To evaluate the different roles of aerosol species in PM pollution, we further compared aerosol compositions between clean periods and polluted episodes (Fig. 10). The average NR-PM_1 mass concentrations varied from 4.0 to 10.4 μg m^{-3} during clean ~~episodes~~periods with much higher concentrations during HP than NHP. Analysis of the compositional differences showed that FFOA and LO-OOA are two species with the largest enhancements during HP, supporting the influences of coal combustion emissions (Fig. 8). Although aerosol bulk composition was relatively similar among different clean ~~episodes~~periods, OA composition showed significant changes from NHP to HP, which are characterized by large increases in FFOA from 7–8% to 14–18%, and LO-OOA from 10–11% to 17–19%. OOA showed corresponding decreases from 60–64% to 44–50%. Aerosol composition was quite different between clean periods and polluted episodes. For example, organics accounted for a higher fraction (55–60%) in NR-PM_1 during clean periods than that (46–54%) in polluted episodes. Higher contribution of organics during clean periods was also previously observed at the same ground site (Sun et al., 2013b). On the contrary, the nitrate contribution showed a large increase in polluted days during NHP and APEC, e.g., 29% vs. 12%, further indicating the predominant role of nitrate in severe haze pollutions particularly ~~in~~during periods free of intense coal combustion. Also note that the differences in nitrate contributions during HP was small between polluted and clean episodes, for example, 16–18% in polluted episodes and 12–15% ~~in~~during clean ~~episodes~~periods. These results suggest that the polluted conditions during HP do not facilitate the nitrate formation substantially. Compared with nitrate, the sulfate mass fractions didn't change much during NHP and HP with slightly higher contributions ~~in~~during clean ~~episodes~~periods, indicating that sulfate was similarly important during both clean periods and polluted episodes. We also noticed nearly twice higher chloride contribution in polluted days compared with clean periods during HP, confirming the increasing role of coal

combustion emissions in severe winter haze pollution.

OA composition was relatively similar between clean periods and polluted episodes during NHP and APEC, and the contributions of POA and SOA were also close between NHP and APEC. This is consistent with our previous conclusion that POA and SOA showed similar reductions at high altitudes during APEC (Chen et al., 2015). The improved ME-2 analysis however showed some changes in POA and SOA composition. For example, the contributions of FFOA and OOA showed increases while COA was decreased during APEC, indicating the impacts of regional emission controls on different types of POA. OA composition during HP showed more differences between clean periods and polluted episodes. As shown in Fig. 10b, LO-OOA and BBOA showed large increases in polluted episodes, for example, from 17–19% to 24–27% for LO-OOA, and from 5–8% to 9–11% for BBOA. However, such changes were not observed during NHP. Therefore, the results here might indicate that the polluted meteorological conditions (high RH and low O_3) during HP facilitate the transformation of combustion-related semi-volatile species into particle phase. In comparison, OOA showed higher contributions to OA in clean periods than polluted episodes during HP. It is interesting that the FFOA and COA contributions at 260 m were comparable between clean periods and polluted episodes, which is largely different from previous observations at ground site where OA comprised much higher COA associated with a large decrease in coal combustion OA during clean periods (Sun et al., 2013b; Sun et al., 2014).

We further calculated the changes of aerosol species during APEC and HP compared with those during NHP. As shown in Fig. 11, almost all species decreased substantially by 40%–70% in polluted days during APEC while the reductions were less significant in clean days when air mass ~~mainly~~ originated mainly from the north-northwest. This is consistent with the fact that strict emission controls were mainly implemented ~~in~~to the south of Beijing during APEC. However, we found an increase in FFOA and much less reductions of SO_2 (~20%) and chloride during APEC compared to other species. One of the major reasons is likely due to the residential coal combustion emissions in Beijing surrounding regions (the average temperature was ~9 ^{o}C) that were transported to the high altitude in urban Beijing during APEC. Consistently, the primary species related to coal combustion emissions e.g., FFOA, SO_2, Chl, and LO-OOA were elevated significantly from NHP to HP although the enhancements were more dramatic in polluted episodes. For example, FFOA was increased by a factor of ~4–5 and the other three species (Chl, LO-OOA and SO_2) by a factor of ~2 in polluted episodes during HP. Our results suggest that coal combustion emission is the major source affecting aerosol composition at high altitudes in heating season. The remarkable enhancement of LO-OOA further supports our conclusion that LO-OOA was likely a combustion related SOA. Comparatively, nitrate and OOA were two species showing the largest decrease during HP mainly due to the reduced photochemical production associated with lower RH and *T*.

3.4 Back trajectory analysis

The response of aerosol chemistry to different source regions was further demonstrated by comparing the aerosol

compositions from similar air masses during the four periods. Figure 12 presents the average chemical compositions of NR-PM_1 species and OA factors corresponding to ~~the~~ four clusters that were determined from the 48 h back trajectories using the Hybrid Single Particle Lagrangian Integrated Trajectory (HYSPLIT, NOAA) model (Draxler and Hess, 1997). The air mass originated from the north/northwest (C1, 40% of the time) but circulated around the south of Beijing showed the highest aerosol ~~loading~~loadings among the four clusters with the average mass concentration of NR-PM_1 ranging from 38.6 to 114.0 μg m^{-3}. Comparatively, the westerly cluster (C2) presented significantly lower aerosol loadings (28.1–62 μg m^{-3}), and the two northwesterly clusters (C3 and C4) showed the lowest mass loadings (< 10 μg m^{-3} for most of the time). Such large differences in aerosol loadings associated with different air masses have been also ~~been~~ reported previously in Beijing (Han et al., 2017), which is consistent with the spatial distributions of emission sources in north China (Zhao et al., 2012). Compared with NHP, C1 from the south showed the largest reductions in NR-PM_1 (56%) during APEC while the reductions were much less for the other three clusters. This is consistent with the fact that strict emission controls were mainly implemented in the regions to the south of Beijing (Chen et al., 2015). These results also highlight that emission control in the south of Beijing is one of the most effective ~~measure~~measures to improve air quality in Beijing. It is interesting to note that the NR-PM_1 showed ubiquitously higher mass concentrations during HP1 and HP2 than NHP once the source regions were synchronized, further supporting the impacts of coal combustion emissions on PM levels. Also, the NR-PM_1 from the most polluted cluster (C1) showed similar levels between HP1 (114 μg m^{-3}) and HP2 (106 μg m^{-3}) while it had more differences (up to a factor of 2) for the other three clusters indicating more source variability from relatively clean regions. The air masses dependent OA mass concentrations were similar to those of NR-PM_1.

NR-PM_1 and OA compositions vary differently among different clusters. For example, nitrate dominated SIA (28–31%) during NHP and APEC in C1 and C2, while sulfate ~~were~~was more prevalent in C3 and C4 (20–24%), indicating the very different ~~emission sources~~source emissions between southerly and northerly air masses. In fact, the regions of C1 and C2 show significantly high NO_x emissions than C3 and C4 (Zhao et al., 2013a). Another possible explanation is the more evaporative loss of nitrate during the long-distance transport in C3 and C4, while sulfate can be transported for a longer distance because it is non-volatile. In addition, less available NH_3 can also be an explanation. However, such nitrate/sulfate differences among different clusters were much reduced during HP1 and HP2 which were likely ~~mainly~~ due to the weaker photochemical production and less evaporative loss under lower *T* in the heating season. OA dominated NR-PM_1 for all clusters, on average accounting for 46–65%. Note that the OA contributions were overall higher in C3 and C4 than C1, indicating an enhanced role of OA in PM during relatively clean periods. Despite the large differences in NR-PM_1 composition, we found that OA composition among different clusters were rather similar. Moreover, all clusters showed similar changes in SOA and POA compositions from NHP to HP. For example, OOA showed large decreases from 55–65% during NHP to 38–57% during HP1 and 27–40% in HP2, while the combustion-related FFOA, BBOA, and LO-OOA all showed corresponding increases during HP. Our results suggest that coal combustion ~~emission~~emissions from different

source regions all can ~~all~~ have great impacts on OA composition in heating season in Beijing.

4 Conclusions

We presented an analysis of submicron aerosols at a high ~~altitude~~height (260 m) in urban Beijing from 10 October 2014 to 18 January 2015. This study contains three periods with different emission scenarios, i.e., NHP, APEC, and HP, providing an experimental opportunity to investigate the response of aerosol chemistry to emission changes at a high ~~altitude~~height. The average mass concentration of NR-PM_1 was 64.9 μg m^{-3} during NHP, and 74.5 and 48.6 μg m^{-3}, respectively during the two different heating periods, i.e., HP1 and HP2. Our results indicate that the average PM level in heating season is not always higher than that in non-heating season. With similar emission sources, e.g., HP1 vs. HP2, meteorological conditions can cause an average difference of NR-PM_1 by 35%, varying from 26 to 44% for different aerosol species. The NR-PM_1 composition was dominated by organics (46%) followed by nitrate (28%) and sulfate (14%) during NHP. However, the nitrate contribution in heating season was decreased substantially from 28% to ~15–18% due to reduced photochemical processing in winter while that of organics was increased to ~51–54%, and chloride was enhanced by a factor of 2 as a result of enhanced coal combustion emissions.

The sources of OA at 260 m were investigated with ME-2 using FFOA, COA, and BBOA resolved at the ground site as constrains. We observed significant changes in both POA and SOA composition from NHP to HP. Not surprising, FFOA showed the largest enhancement from 5% to 13–21% as a result of enhanced coal combustion emissions. Comparatively, OOA decreased substantially from 56% to 32–40% during HP. The less oxidized OOA however showed a remarkable increase from 9–16% to 24–26%. Our results illustrated the different properties of the two types of SOA at 260 m. While OOA was dominantly from photochemical production, LO-OOA was more likely a combustion-related SOA, consistent with the tight correlations with chloride and CO during HP. We also found a considerable contribution of COA at high ~~altitude~~height (10–13%) although it was nearly twice lower than that at ground site. Overall, SOA dominated OA at 260 m, on average accounting for 72% in non-heating season and 58 –64% in heating season. Compared with ground measurements, SOA showed much higher contributions at 260 m by 15–34%, demonstrating the importance of SOA in PM pollution at high altitudes in the city. Our results illustrated the large differences in POA and SOA between ground level and 260 m which have significant implications that measurements at high altitudes are critical to better validate the simulations of POA and SOA in chemical transport models.

Data availability. The data in this study are available from the authors upon request (sunyele@mail.iap.ac.cn).

Competing interests. The authors declare that they have no conflict of interest.

Acknowledgments

. This work was supported by the National Key Project of Basic Research (2014CB447900), the Beijing Natural Science Foundation (8161004), and the National Natural Science Foundation of China (41571130034, 41575120).

References

Aiken, A. C., DeCarlo, P. F., Kroll, J. H., Worsnop, D. R., Huffman, J. A., Docherty, K. S., Ulbrich, I. M., Mohr, C., Kimmel, J. R., Sueper, D., Sun, Y., Zhang, Q., Trimborn, A., Northway, M., Ziemann, P. J., Canagaratna, M. R., Onasch, T. B., Alfarra, M. R., Prevot, A. S. H., Dommen, J., Duplissy, J., Metzger, A., Baltensperger, U., and Jimenez, J. L.: O/C and OM/OC Ratios of Primary, Secondary, and Ambient Organic Aerosols with High-Resolution Time-of-Flight Aerosol Mass Spectrometry, Environ. Sci. Technol., 42, 4478–4485, doi:10.1021/es703009q, 2008.

Aiken, A. C., Salcedo, D., Cubison, M. J., Huffman, J. A., DeCarlo, P. F., Ulbrich, I. M., Docherty, K. S., Sueper, D., Kimmel, J. R., Worsnop, D. R., Trimborn, A., Northway, M., Stone, E. A., Schauer, J. J., Volkamer, R. M., Fortner, E., de Foy, B., Wang, J., Laskin, A., Shutthanandan, V., Zheng, J., Zhang, R., Gaffney, J., Marley, N. A., Paredes-Miranda, G., Arnott, W. P., Molina, L. T., Sosa, G., and Jimenez, J. L.: Mexico City aerosol analysis during MILAGRO using high resolution aerosol mass spectrometry at the urban supersite (T0)–Part 1: Fine particle composition and organic source apportionment, Atmos. Chem. Phys., 9, 6633–6653, doi:10.5194/acp-9-6633-2009, 2009.

Allan, J. D., Williams, P. I., Morgan, W. T., Martin, C. L., Flynn, M. J., Lee, J., Nemitz, E., Phillips, G. J., Gallagher, M. W., and Coe, H.: Contributions from transport, solid fuel burning and cooking to primary organic aerosols in two UK cities, Atmos. Chem. Phys., 10, 647–668, doi:10.5194/acp-10-647-2010, 2010.

Canonaco, F., Crippa, M., Slowik, J. G., Baltensperger, U., and Prévôt, A. S. H.: SoFi, an IGOR-based interface for the efficient use of the generalized multilinear engine (ME-2) for the source apportionment: ME-2 application to aerosol mass spectrometer data, Atmos. Meas. Tech., 6, 3649–3661, doi:10.5194/amt-6-3649-2013, 2013.

Chen, C., Sun, Y. L., Xu, W. Q., Du, W., Zhou, L. B., Han, T. T., Wang, Q. Q., Fu, P. Q., Wang, Z. F., Gao, Z. Q., Zhang, Q., and Worsnop, D. R.: Characteristics and sources of submicron aerosols above the urban canopy (260 m) in Beijing, China, during the 2014 APEC summit, Atmos. Chem. Phys., 15, 12879–12895, doi:10.5194/acp-15-12879-2015, 2015.

Cheng, Y., Zheng, G., Wei, C., Mu, Q., Zheng, B., Wang, Z., Gao, M., Zhang, Q., He, K., Carmichael, G., Pöschl, U., and Su, H.: Reactive nitrogen chemistry in aerosol water as a source of sulfate during haze events in China, Sci. Adv., 2, doi:10.1126/sciadv.1601530, 2016.

Crenn, V., Sciare, J., Croteau, P. L., Verlhac, S., Fröhlich, R., Belis, C. A., Aas, W., Äijälä, M., Alastuey, A., Artiñano, B., Baisnée, D., Bonnaire, N., Bressi, M., Canagaratna, M., Canonaco, F., Carbone, C., Cavalli, F., Coz, E., Cubison, M. J., Esser-Gietl, J. K., Green, D. C., Gros, V., Heikkinen, L., Herrmann, H., Lunder, C., Minguillón, M. C., Močnik, G., O'Dowd, C. D., Ovadnevaite, J., Petit, J. E., Petralia, E., Poulain, L., Priestman, M., Riffault, V., Ripoll, A., Sarda-Estève, R., Slowik, J. G., Setyan, A., Wiedensohler, A., Baltensperger, U., Prévôt, A. S. H., Jayne, J. T., and Favez, O.: ACTRIS ACSM intercomparison – Part 1: Reproducibility of concentration and fragment results from 13 individual Quadrupole Aerosol Chemical Speciation Monitors (Q-ACSM) and consistency with co-located instruments,

Atmos. Meas. Tech., 8, 5063-5087, 10.5194/amt-8-5063-2015, 2015.

Crippa, M., DeCarlo, P. F., Slowik, J. G., Mohr, C., Heringa, M. F., Chirico, R., Poulain, L., Freutel, F., Sciare, J., Cozic, J., Di Marco, C. F., Elsasser, M., Nicolas, J. B., Marchand, N., Abidi, E., Wiedensohler, A., Drewnick, F., Schneider, J., Borrmann, S., Nemitz, E., Zimmermann, R., Jaffrezo, J. L., Prévôt, A. S. H., and Baltensperger, U.: Wintertime aerosol chemical composition and source apportionment of the organic fraction in the metropolitan area of Paris, Atmos. Chem. Phys., 13, 961–981, doi:10.5194/acp-13-961-2013, 2013.

Crippa, M., Canonaco, F., Lanz, V. A., Äijälä, M., Allan, J. D., Carbone, S., Capes, G., Ceburnis, D., Dall'Osto, M., Day, D. A., DeCarlo, P. F., Ehn, M., Eriksson, A., Freney, E., Hildebrandt Ruiz, L., Hillamo, R., Jimenez, J. L., Junninen, H., Kiendler-Scharr, A., Kortelainen, A. M., Kulmala, M., Laaksonen, A., Mensah, A. A., Mohr, C., Nemitz, E., O'Dowd, C., Ovadnevaite, J., Pandis, S. N., Petäjä, T., Poulain, L., Saarikoski, S., Sellegri, K., Swietlicki, E., Tiitta, P., Worsnop, D. R., Baltensperger, U., and Prévôt, A. S. H.: Organic aerosol components derived from 25 AMS data sets across Europe using a consistent ME-2 based source apportionment approach, Atmos. Chem. Phys., 14, 6159–6176, doi:10.5194/acp-14-6159-2014, 2014.

Dockery , D. W., Pope , C. A., Xu , X., Spengler , J. D., Ware , J. H., Fay , M. E., Ferris , B. G. J., and Speizer , F. E.: An Association between Air Pollution and Mortality in Six U.S. Cities, New Engl. J. Med., 329, 1753–1759, doi:10.1056/nejm199312093292401, 1993.

Draxler, R. R., and Hess, G.: Description of the HYSPLIT4 modeling system, 1997.

Elser, M., Huang, R.-J., Wolf, R., Slowik, J. G., Wang, Q., Canonaco, F., Li, G., Bozzetti, C., Daellenbach, K. R., Huang, Y., Zhang, R., Li, Z., Cao, J., Baltensperger, U., El-Haddad, I., and Prévôt, A. S. H.: New insights into $PM_{2.5}$ chemical composition and sources in two major cities in China during extreme haze events using aerosol mass spectrometry, Atmos. Chem. Phys., 16, 3207-3225, doi:10.5194/acp-16-3207-2016, 2016.

Guo, S., Hu, M., Zamora, M. L., Peng, J., Shang, D., Zheng, J., Du, Z., Wu, Z., Shao, M., Zeng, L., Molina, M. J., and Zhang, R.: Elucidating severe urban haze formation in China, P. Natl. Acad. Sci. USA,, 111, 17373–17378, doi:10.1073/pnas.1419604111, 2014.

Han, T., Xu, W., Li, J., Freedman, A., Zhao, J., Wang, Q., Chen, C., Zhang, Y., Wang, Z., Fu, P., Liu, X., and Sun, Y.: Aerosol optical properties measurements by a CAPS single scattering albedo monitor: Comparisons between summer and winter in Beijing, China, J. Geophys. Res.-Atmos., 122, 2513–2526, doi:10.1002/2016JD025762, 2017.

Huang, R.-J., Zhang, Y., Bozzetti, C., Ho, K.-F., Cao, J.-J., Han, Y., Daellenbach, K. R., Slowik, J. G., Platt, S. M., Canonaco, F., Zotter, P., Wolf, R., Pieber, S. M., Bruns, E. A., Crippa, M., Ciarelli, G., Piazzalunga, A., Schwikowski, M., Abbaszade, G., Schnelle-Kreis, J., Zimmermann, R., An, Z., Szidat, S., Baltensperger, U., Haddad, I. E., and Prevot, A. S. H.: High secondary aerosol contribution to particulate pollution during haze events in China, Nature, 514, 218–222, doi:10.1038/nature13774, 2014.

Huang, X. F., He, L. Y., Hu, M., Canagaratna, M. R., Sun, Y., Zhang, Q., Zhu, T., Xue, L., Zeng, L. W., Liu, X. G., Zhang, Y. H., Jayne, J. T., Ng, N. L., and Worsnop, D. R.: Highly time-resolved chemical characterization of atmospheric submicron particles during 2008 Beijing Olympic Games using an Aerodyne High-Resolution Aerosol Mass Spectrometer, Atmos. Chem. Phys., 10, 8933–8945, doi:10.5194/acp-10-8933-2010, 2010.

IPCC: Intergovernmental Panel on Climate Change (2013), Climate Change 2013: The Physical Science Basis. Contribution of Working Group I to the Fifth Assessment Report of the Intergovernmental Panel on Climate Change, 2013.

Jimenez, J., Canagaratna, M., Donahue, N., Prevot, A., Zhang, Q., Kroll, J., DeCarlo, P., Allan, J., Coe, H., and Ng, N.: Evolution of organic aerosols in the atmosphere, Science, 326, 1525–1529, doi:10.1126/science.1180353, 2009.

Li, H., Zhang, Q., Zhang, Q., Chen, C., Wang, L., Wei, Z., Zhou, S., Parworth, C., Zheng, B., Canonaco, F., Prévôt, A. S. H., Chen, P., Zhang, H., Wallington, T. J., and He, K.: Wintertime aerosol chemistry and haze evolution in an extremely polluted city of the North China Plain: significant contribution from coal and biomass combustion, Atmos. Chem. Phys., 17, 4751–4768, doi:10.5194/acp-17-4751-2017, 2017.

Lin, C., Ceburnis, D., Hellebust, S., Buckley, P., Wenger, J., Canonaco, F., Prevot, A. S. H., Huang, R. J., O'Dowd, C., and Ovadnevaite, J.: Characterization of Primary Organic Aerosol from Domestic Wood, Peat, and Coal Burning in Ireland, Environ. Sci. Technol., doi:10.1021/acs.est.7b01926, 2017.

Ma, Q., Cai, S., Wang, S., Zhao, B., Martin, R. V., Brauer, M., Cohen, A., Jiang, J., Zhou, W., Hao, J., Frostad, J., Forouzanfar, M. H., and Burnett, R. T.: Impacts of coal burning on ambient $PM_{2.5}$ pollution in China, Atmos. Chem. Phys., 17, 4477–4491, doi:10.5194/acp-17-4477-2017, 2017.

Matthew, B. M., Middlebrook, A. M., and Onasch, T. B.: Collection Efficiencies in an Aerodyne Aerosol Mass Spectrometer as a Function of Particle Phase for Laboratory Generated Aerosols, Aerosol Sci. Tech., 42, 884–98, doi:10.1080/02786820802356797, 2008.

Middlebrook, A. M., Bahreini, R., Jimenez, J. L., and Canagaratna, M. R.: Evaluation of Composition-Dependent Collection Efficiencies for the Aerodyne Aerosol Mass Spectrometer using Field Data, Aerosol Sci. Tech., 46, 258–271, doi:10.1080/02786826.2011.620041, 2012.

Mohr, C., DeCarlo, P. F., Heringa, M. F., Chirico, R., Slowik, J. G., Richter, R., Reche, C., Alastuey, A., Querol, X., Seco, R., Peñuelas, J., Jiménez, J. L., Crippa, M., Zimmermann, R., Baltensperger, U., and Prévôt, A. S. H.: Identification and quantification of organic aerosol from cooking and other sources in Barcelona using aerosol mass spectrometer data, Atmos. Chem. Phys., 12, 1649–1665, doi:10.5194/acp-12-1649-2012, 2012.

Ng, N. L., Canagaratna, M. R., Jimenez, J. L., Zhang, Q., Ulbrich, I. M., and Worsnop, D. R.: Real-Time Methods for Estimating Organic Component Mass Concentrations from Aerosol Mass Spectrometer Data, Environ. Sci. Technol., 45, 910–916, doi:10.1021/es102951k, 2011.

Ohta, S., and Okita, T.: A chemical characterization of atmospheric aerosol in Sapporo, Atmos. Environ., 24, 815–822, doi:org/10.1016/0960-1686(90)90282-R, 1990.

Ots, R., Vieno, M., Allan, J. D., Reis, S., Nemitz, E., Young, D. E., Coe, H., Di Marco, C., Detournay, A., Mackenzie, I. A., Green, D. C., and Heal, M. R.: Model simulations of cooking organic aerosol (COA) over the UK using estimates of emissions based on measurements at two sites in London, Atmos. Chem. Phys., 16, 13773–13789, doi:10.5194/acp-16-13773-2016, 2016.

Paatero, and Tapper, a.: Positive and matrix factorization: A non-negative factor model with optimal utilization of error estimates of data values, Environmetrics, 5, 111-126, 1994.

Sun, Y. L., Zhang, Q., Schwab, J. J., Demerjian, K. L., Chen, W. N., Bae, M. S., Hung, H. M., Hogrefe, O., Frank, B., Rattigan, O. V., and Lin, Y. C.: Characterization of the sources and processes of organic and inorganic aerosols in New York City with a high-resolution time-of-flight aerosol mass spectrometer, Atmos. Chem. Phys., 11, 1581-1602, 10.5194/acp-11-1581-2011, 2011.

Sun, Y., Wang, Z., Fu, P., Jiang, Q., Yang, T., Li, J., and Ge, X.: The impact of relative humidity on aerosol composition and evolution processes during wintertime in Beijing, China, Atmos. Environ., 77, 927–934, doi:10.1016/j.atmosenv.2013.06.019, 2013a.

Sun, Y., Jiang, Q., Wang, Z., Fu, P., Li, J., Yang, T., and Yin, Y.: Investigation of the sources and evolution processes of severe haze pollution in Beijing in January 2013, J. Geophys. Res.-Atmos., 119, 4380–4398, doi:10.1002/2014jd021641, 2014.

Sun, Y., Du, W., Wang, Q., Zhang, Q., Chen, C., Chen, Y., Chen, Z., Fu, P., Wang, Z., Gao, Z., and Worsnop, D. R.: Real-Time Characterization of Aerosol Particle Composition above the Urban Canopy in Beijing: Insights into the Interactions between the Atmospheric Boundary Layer and Aerosol Chemistry, Environ. Sci. Technol., 49, 11340–11347, doi:10.1021/acs.est.5b02373, 2015a.

Sun, Y., Chen, C., Zhang, Y., Xu, W., Zhou, L., Cheng, X., Zheng, H., Ji, D., Li, J., Tang, X., Fu, P., and Wang, Z.: Rapid formation and evolution of an extreme haze episode in Northern China during winter 2015, Sci. Rep., 6, 27151, doi:10.1038/srep27151, 2016a.

Sun, Y., Du, W., Fu, P., Wang, Q., Li, J., Ge, X., Zhang, Q., Zhu, C., Ren, L., Xu, W., Zhao, J., Han, T., Worsnop, D. R., and Wang, Z.: Primary and secondary aerosols in Beijing in winter: sources, variations and processes, Atmos. Chem. Phys., 16, 8309–8329, doi:10.5194/acp-16-8309-2016, 2016b.

Sun, Y., Wang, Z., Wild, O., Xu, W., Chen, C., Fu, P., Du, W., Zhou, L., Zhang, Q., Han, T., Wang, Q., Pan, X., Zheng, H., Li, J., Guo, X., Liu, J., and Worsnop, D. R.: "APEC Blue": Secondary Aerosol Reductions from Emission Controls in Beijing, Sci. Rep., 6, 20668, doi:10.1038/srep20668, 2016c.

Sun, Y. L., Zhang, Q., Schwab, J. J., Chen, W. N., Bae, M. S., Hung, H. M., Lin, Y. C., Ng, N. L., Jayne, J., Massoli, P.,

Williams, L. R., and Demerjian, K. L.: Characterization of near-highway submicron aerosols in New York City with a high-resolution aerosol mass spectrometer, Atmos. Chem. Phys., 12, 2215–2227, doi:10.5194/acp-12-2215-2012, 2012.

Sun, Y. L., Wang, Z. F., Fu, P. Q., Yang, T., Jiang, Q., Dong, H. B., Li, J., and Jia, J. J.: Aerosol composition, sources and processes during wintertime in Beijing, China, Atmos. Chem. Phys., 13, 4577–4592, doi:10.5194/acp-13-4577-2013, 2013b.

Sun, Y. L., Wang, Z. F., Du, W., Zhang, Q., Wang, Q. Q., Fu, P. Q., Pan, X. L., Li, J., Jayne, J., and Worsnop, D. R.: Long-term real-time measurements of aerosol particle composition in Beijing, China: seasonal variations, meteorological effects, and source analysis, Atmos. Chem. Phys., 15, 10149–10165, doi:10.5194/acp-15-10149-2015, 2015b.

Ulbrich, I. M., Canagaratna, M. R., Zhang, Q., Worsnop, D. R., and Jimenez, J. L.: Interpretation of organic components from Positive Matrix Factorization of aerosol mass spectrometric data, Atmos. Chem. Phys., 9, 2891–2918, doi:10.5194/acp-9-2891-2009, 2009.

Wang, Q., Sun, Y., Jiang, Q., Du, W., Sun, C., Fu, P., and Wang, Z.: Chemical composition of aerosol particles and light extinction apportionment before and during the heating season in Beijing, China, J. Geophys. Res.-Atmos., 120, 12708–12722, doi:10.1002/2015JD023871, 2015.

Wang, Q., Zhao, J., Du, W., Ana, G., Wang, Z., Sun, L., Wang, Y., Zhang, F., Li, Z., Ye, X., and Sun, Y.: Characterization of submicron aerosols at a suburban site in central China, Atmos. Environ., 131, 115–123, doi:10.1016/j.atmosenv.2016.01.054, 2016.

Wu, P., Ding, Y., and Liu, Y.: Atmospheric circulation and dynamic mechanism for persistent haze events in the Beijing–Tianjin–Hebei region, Adv. Atmos. Sci., 34, 429–440, doi:10.1007/s00376-016-6158-z, 2017.

Xu, J., Zhang, Q., Chen, M., Ge, X., Ren, J., and Qin, D.: Chemical composition, sources, and processes of urban aerosols during summertime in northwest China: insights from high-resolution aerosol mass spectrometry, Atmos. Chem. Phys., 14, 12593–12611, doi:10.5194/acp-14-12593-2014, 2014.

Xu, W., Han, T., Du, W., Wang, Q., Chen, C., Zhao, J., Zhang, Y., Li, J., Fu, P., Wang, Z., Worsnop, D. R., and Sun, Y.: Effects of Aqueous-Phase and Photochemical Processing on Secondary Organic Aerosol Formation and Evolution in Beijing, China, Environ. Sci. Technol., 51, 762–770, doi:10.1021/acs.est.6b04498, 2017.

Xu, W. Q., Sun, Y. L., Chen, C., Du, W., Han, T. T., Wang, Q. Q., Fu, P. Q., Wang, Z. F., Zhao, X. J., Zhou, L. B., Ji, D. S., Wang, P. C., and Worsnop, D. R.: Aerosol composition, oxidation properties, and sources in Beijing: results from the 2014 Asia-Pacific Economic Cooperation summit study, Atmos. Chem. Phys., 15, 13681–13698, doi:10.5194/acp-15-13681-2015, 2015.

Yang, Y. R., Liu, X. G., Qu, Y., An, J. L., Jiang, R., Zhang, Y. H., Sun, Y. L., Wu, Z. J., Zhang, F., Xu, W. Q., and Ma, Q. X.:

Characteristics and formation mechanism of continuous hazes in China: a case study during the autumn of 2014 in the North China Plain, Atmos. Chem. Phys., 15, 8165–8178, doi:10.5194/acp-15-8165-2015, 2015.

Zhang, J. K., Sun, Y., Liu, Z. R., Ji, D. S., Hu, B., Liu, Q., and Wang, Y. S.: Characterization of submicron aerosols during a month of serious pollution in Beijing, 2013, Atmos. Chem. Phys., 14, 2887–2903, doi:10.5194/acp-14-2887-2014, 2014.

Zhang, J. K., Cheng, M. T., Ji, D. S., Liu, Z. R., Hu, B., Sun, Y., and Wang, Y. S.: Characterization of submicron particles during biomass burning and coal combustion periods in Beijing, China, Sci. Total. Environ., 562, 812–821, doi:10.1016/j.scitotenv.2016.04.015, 2016a.

Zhang, Q., Jimenez, J. L., Canagaratna, M. R., Allan, J. D., Coe, H., Ulbrich, I., Alfarra, M. R., Takami, A., Middlebrook, A. M., Sun, Y. L., Dzepina, K., Dunlea, E., Docherty, K., DeCarlo, P. F., Salcedo, D., Onasch, T., Jayne, J. T., Miyoshi, T., Shimono, A., Hatakeyama, S., Takegawa, N., Kondo, Y., Schneider, J., Drewnick, F., Borrmann, S., Weimer, S., Demerjian, K., Williams, P., Bower, K., Bahreini, R., Cottrell, L., Griffin, R. J., Rautiainen, J., Sun, J. Y., Zhang, Y. M., and Worsnop, D. R.: Ubiquity and dominance of oxygenated species in organic aerosols in anthropogenically-influenced Northern Hemisphere midlatitudes, Geophys. Res. Lett., 34, L13801, doi:10.1029/2007gl029979, 2007.

Zhang, Y., Sun, Y., Du, W., Wang, Q., Chen, C., Han, T., Lin, J., Zhao, J., Xu, W., Gao, J., Li, J., Fu, P., Wang, Z., and Han, Y.: Response of aerosol composition to different emission scenarios in Beijing, China, Sci. Total. Environ., 571, 902–908, doi:10.1016/j.scitotenv.2016.07.073, 2016b.

Zhao, B., Wang, P., Ma, J. Z., Zhu, S., Pozzer, A., and Li, W.: A high-resolution emission inventory of primary pollutants for the Huabei region, China, Atmos. Chem. Phys., 12, 481–501, doi:10.5194/acp-12-481-2012, 2012.

Zhao, B., Wang, S. X., Liu, H., Xu, J. Y., Fu, K., Klimont, Z., Hao, J. M., He, K. B., Cofala, J., and Amann, M.: NOx emissions in China: historical trends and future perspectives, Atmos. Chem. Phys., 13, 9869–9897, doi:10.5194/acp-13-9869-2013, 2013a.

Zhao, J., Du, W., Zhang, Y., Wang, Q., Chen, C., Xu, W., Han, T., Wang, Y., Fu, P., Wang, Z., Li, Z., and Sun, Y.: Insights into aerosol chemistry during the 2015 China Victory Day parade: results from simultaneous measurements at ground level and 260 m in Beijing, Atmos. Chem. Phys., 17, 3215–3232, doi:10.5194/acp-17-3215-2017, 2017.

Zhao, X. J., Zhao, P. S., Xu, J., Meng, W., Pu, W. W., Dong, F., He, D., and Shi, Q. F.: Analysis of a winter regional haze event and its formation mechanism in the North China Plain, Atmos. Chem. Phys., 13, 5685–5696, doi:10.5194/acp-13-5685-2013, 2013b.

Table 1: Summary of the average meteorological parameters, NR-PM_1 species, OA factors and gaseous species ~~for~~during four different periods (i.e., NHP, APEC, HP1 and HP2).

	NHP	APEC	HP1	HP2
Meteorological parameters				
RH	47.1	29.9	42.7	29.1
T	13.3	9.0	5.3	-0.3
WS	4.2	4.8	3.7	5.0
NR-PM_1 species (μg m^{-3})				
NR-PM_1	64.9	25.0	74.5	48.6
Org	30.1	12.2	37.9	26.5
SO_4	8.8	2.5	11.2	6.9
NO_3	17.9	7.1	13.3	7.4
NH_4	5.7	2.2	5.8	4.3
Chl	2.5	1.1	6.3	3.6
OA (μg m^{-3})				
FFOA	1.4	1.2	4.7	5.2
COA	3.7	1.2	4.8	2.7
BBOA	3.0	0.8	3.2	2.7
LO-OOA	4.6	1.1	8.5	6.6
OOA	16.1	7.2	14.3	8.0
Gaseous species				
CO (ppm)	N/A	N/A	3.8	2.5
SO_2 (ppb)	8.0	6.3	12.6	13.9

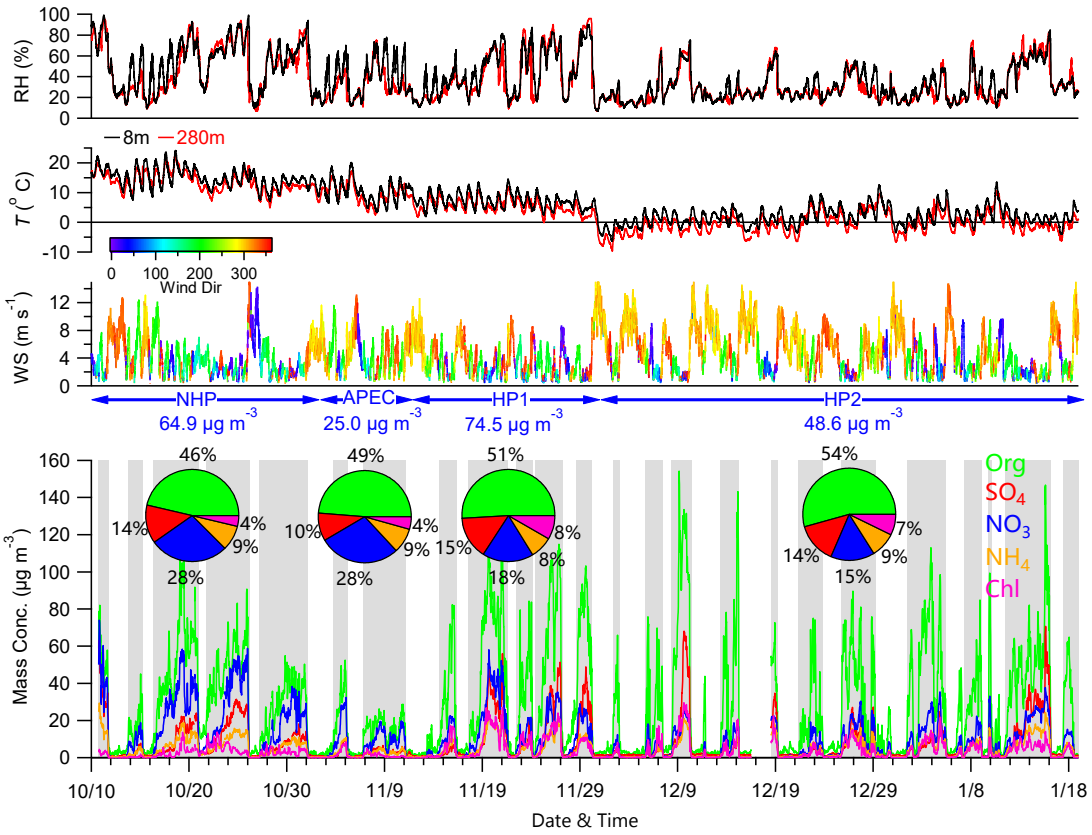

Figure 1: Time series of meteorological parameters (RH, *T*, WS and WD) and mass concentrations of NR-PM$_1$ species (Org, SO_4, NO_3, NH_4, Chl). The four pie charts show the average chemical composition during the four different periods, i.e., NHP, APEC, HP1, and HP2, respectively. The polluted episodes are marked in grey for further discussions, and the rest of the time are defined as clean periods.

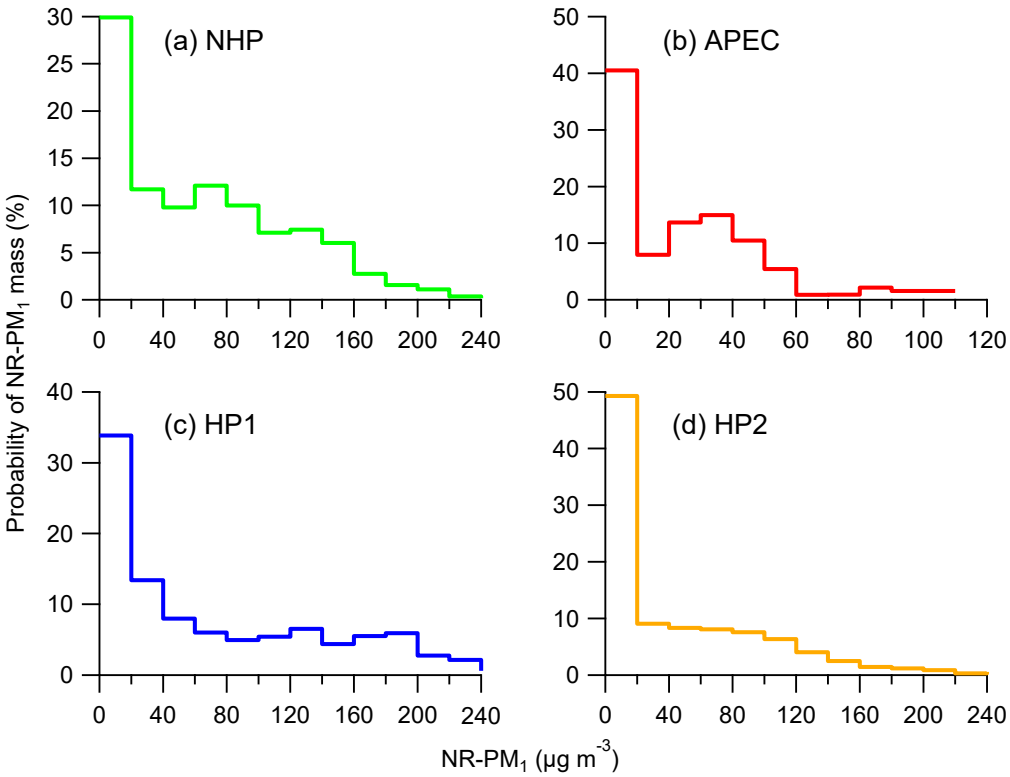

Figure 2: Probability of NR-PM_1 mass during four different periods (a-d), i.e., NHP, APEC, HP1, and HP2.

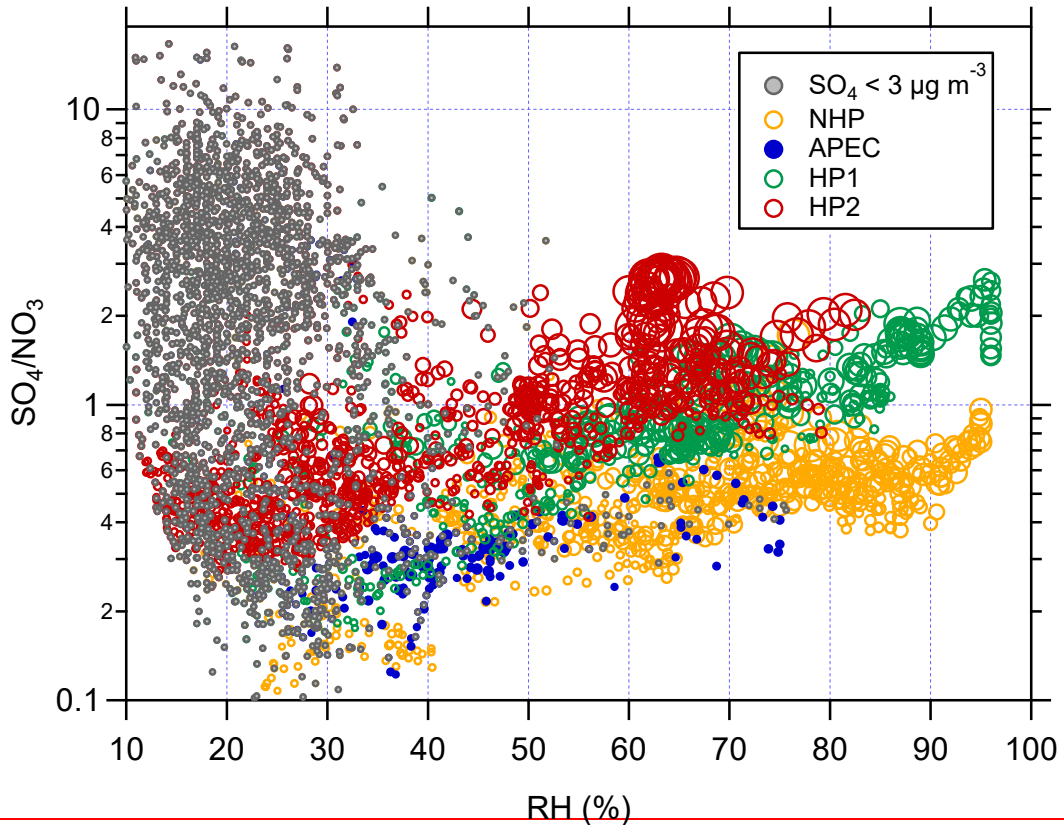
SO4 < 3 μg m-3
NHP
APEC
HP1
HP2
SO4/NO3
RH (%)
10
8
6
4
2
1
0.1
10
20
30
40
50
60
70
80
90
100

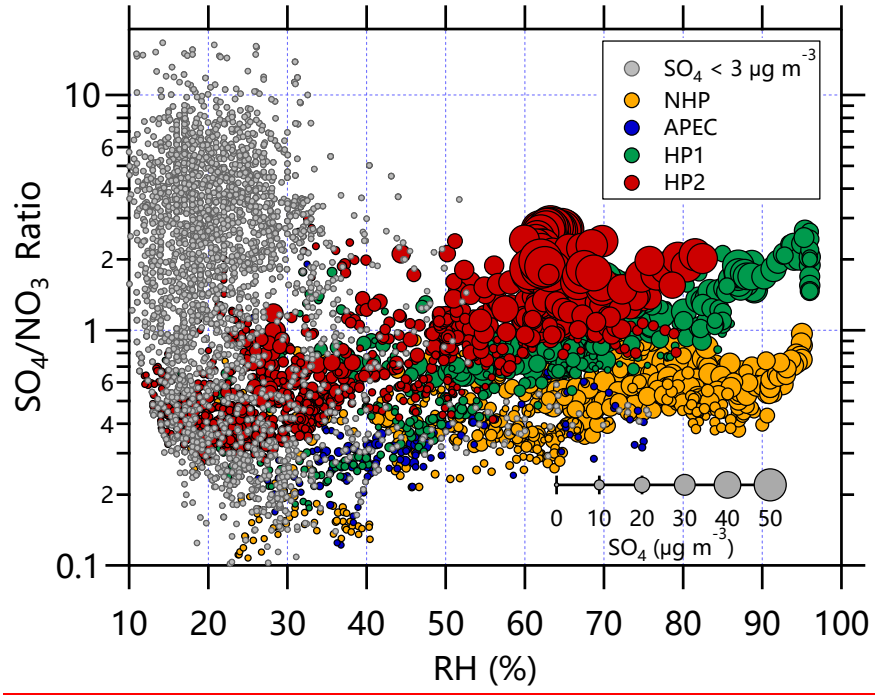

Figure 3: The variations of SO_4/NO_3 ~~ratio~~ratios as a function of RH during four different periods, i.e., NHP, APEC, HP1, and HP2. The marker sizes indicate the SO_4 concentrations, and the data points with the SO_4 concentrations less than 3 ~~μg~~μg m^{-3} are marked in grey.

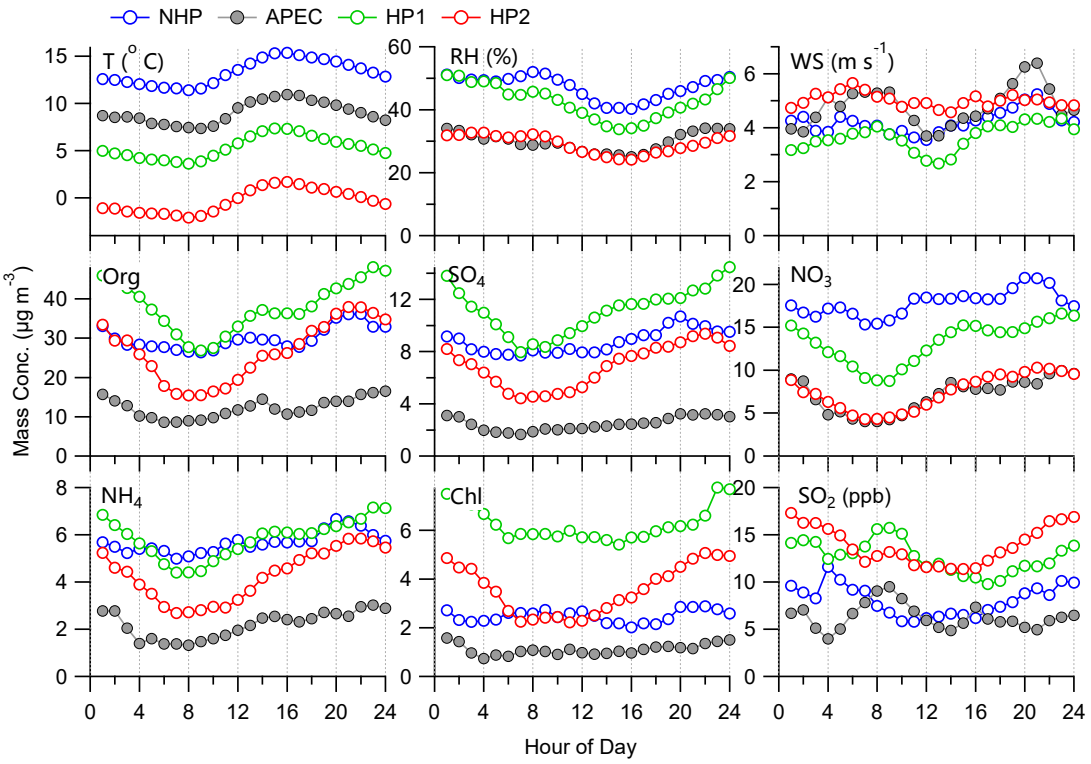

Figure 4: Diurnal variations of meteorological parameters (RH, *T*, WS), NR-PM_1 species and SO_2 during the four different periods, i.e., NHP, APEC, HP1, and HP2.

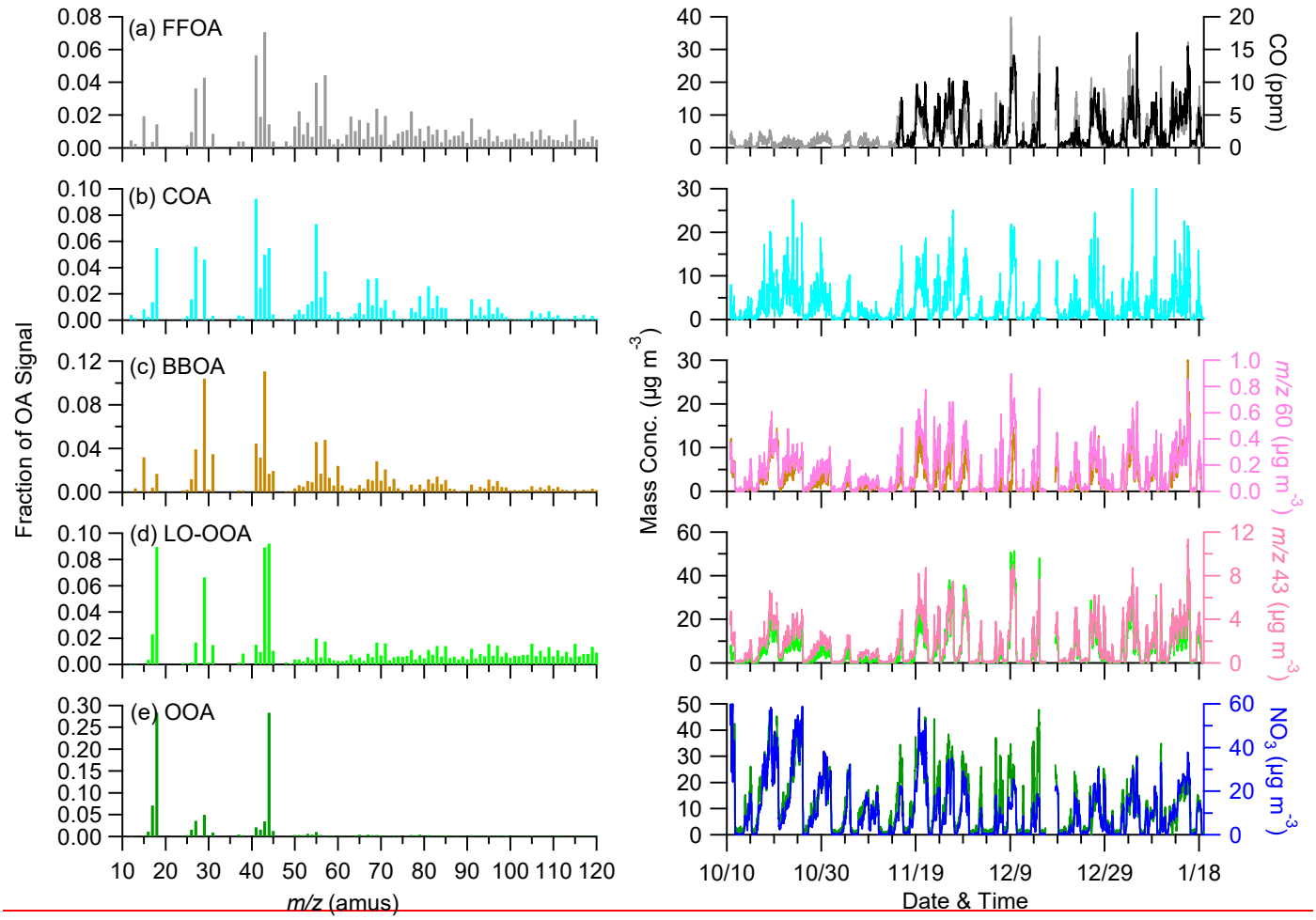
(a) FFOA
(b) COA
(c) BBOA
(d) LO-OOA
(e) OOA
Fraction of OA Signal
m/z (amus)
Mass Conc. (μg m-3)
CO (ppm)
m/z 60 (μg m-3)
m/z 43 (μg m-3)
NO3 (μg m-3)
Date & Time
10/10
10/30
11/19
12/9
12/29
1/18

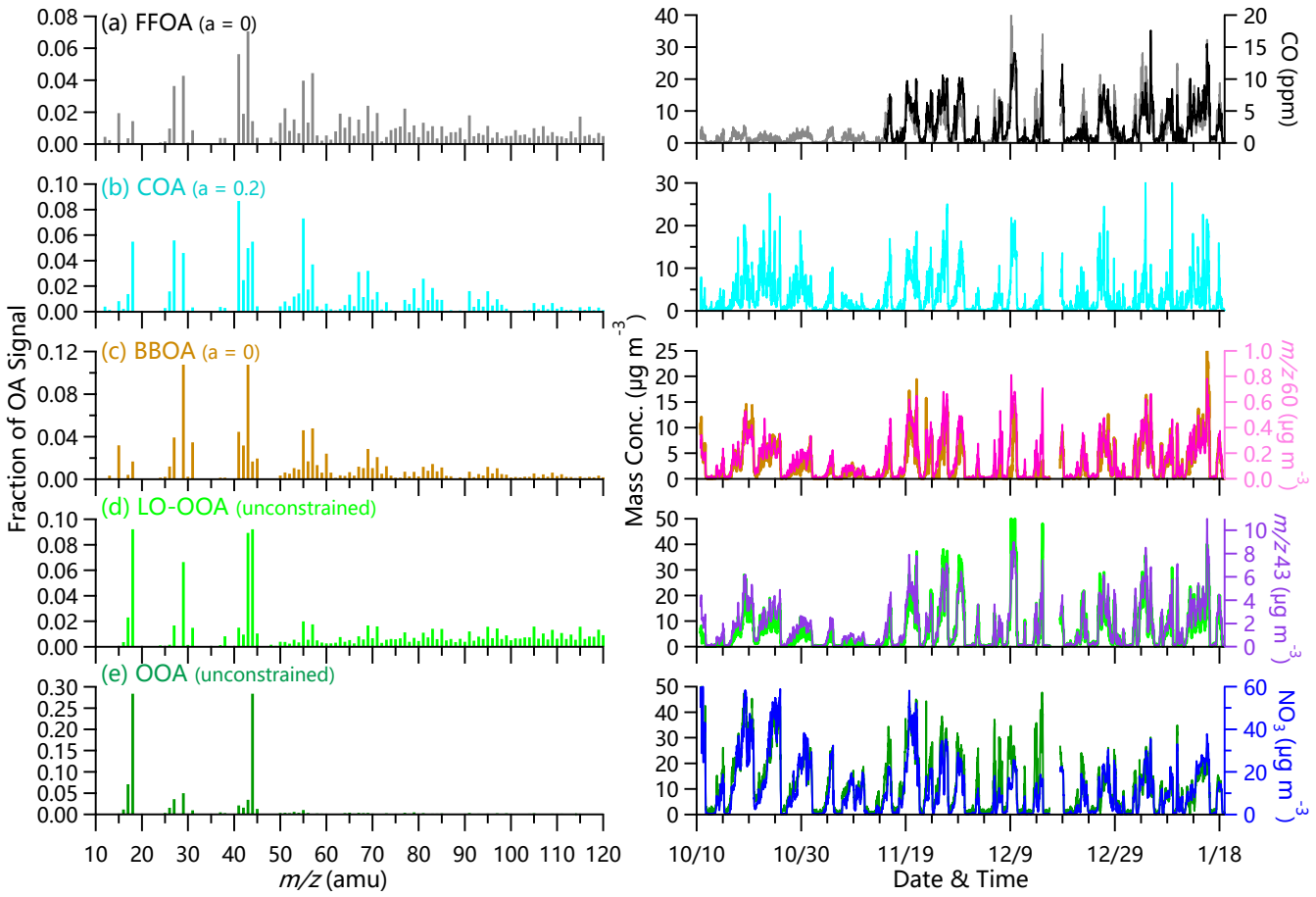

Figure 5: Mass spectra (left panel) and time series (right panel) of five organic aerosol (OA) factors including (a) fossil fuel-related OA (FFOA), (b) cooking OA (COA), (c) biomass-burning OA (BBOA), (d) less oxidized oxygenated OA (LO-OOA), and (e) oxygenated OA (OOA). Also shown in the right panel are the time series of other tracers including CO, nitrate, *m/z* 60, and *m/z* 43 ~~and nitrate~~.

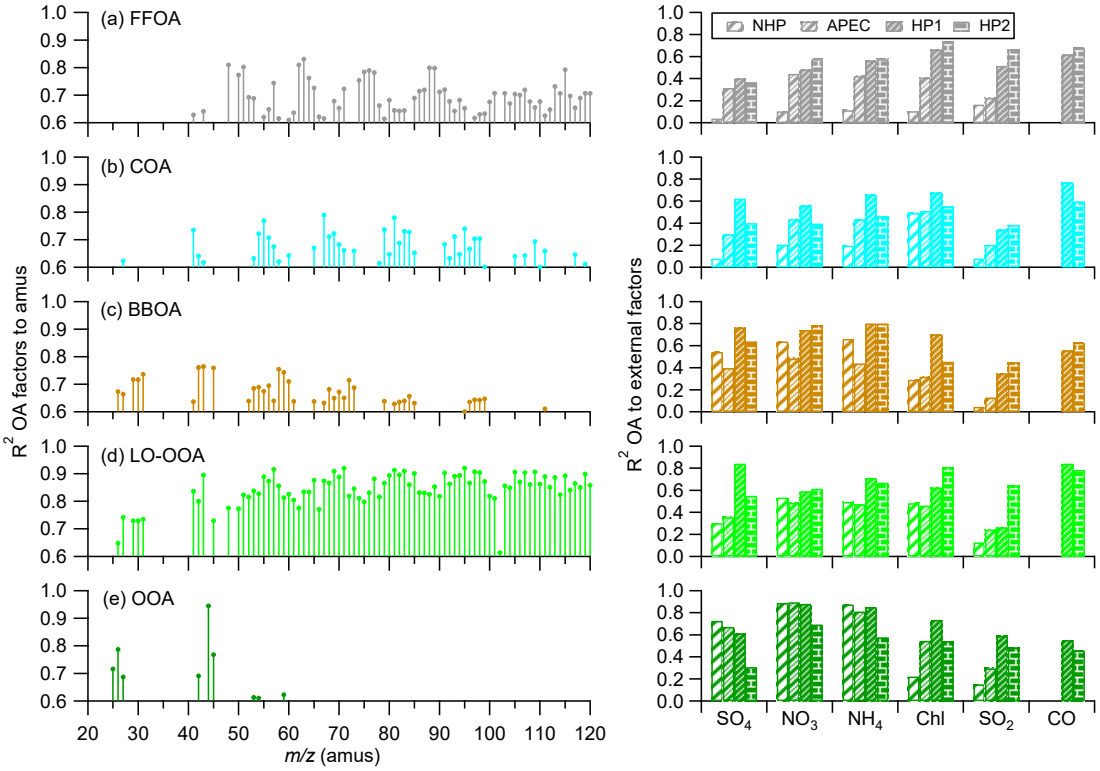

Figure 6: ~~The correlations~~Correlations between the five OA factors and *m/z*'s (left panel) and external tracer species (right panel) during the four different periods, i.e., NHP, APEC, HP1, and HP2.

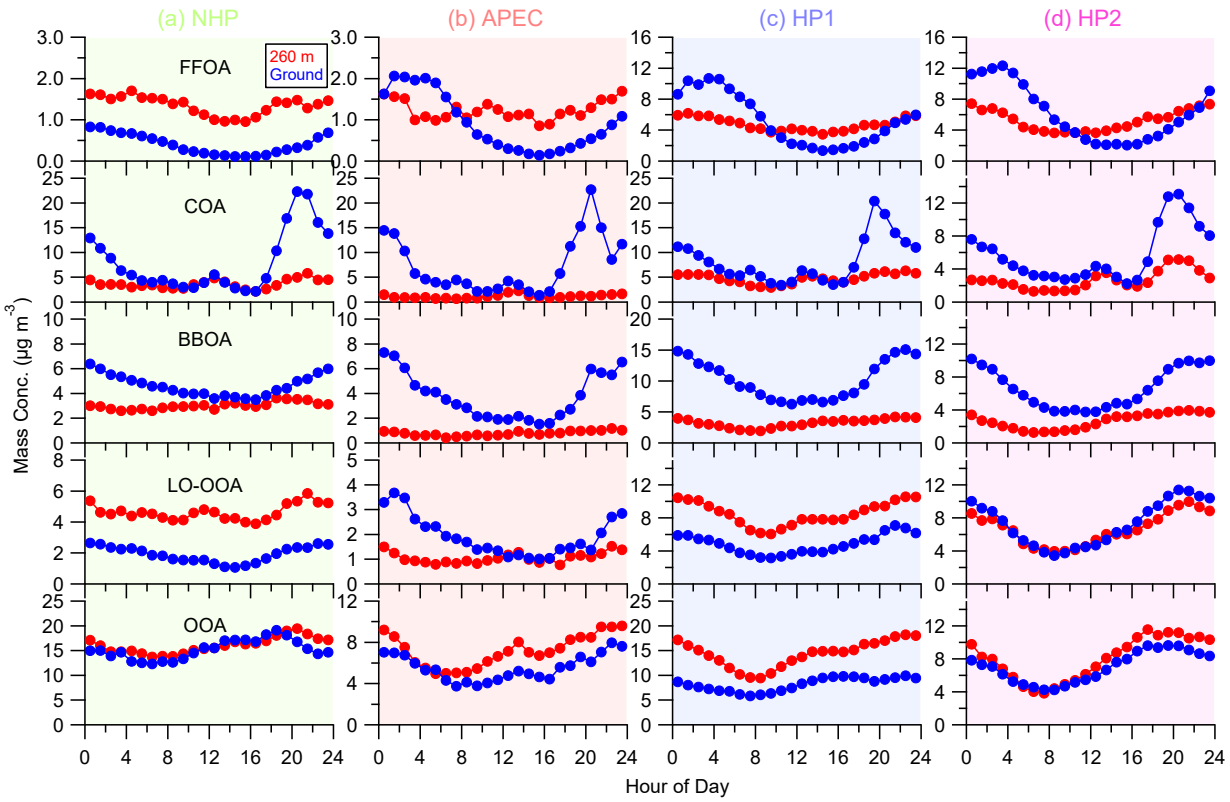

Figure 7: Diurnal ~~evolutions~~cycles of OA factors ~~measured during the four different periods (a–d), i.e., NHP, APEC, HP1, and HP2. The OA factors resolved at ground site are also shown for comparisons~~.

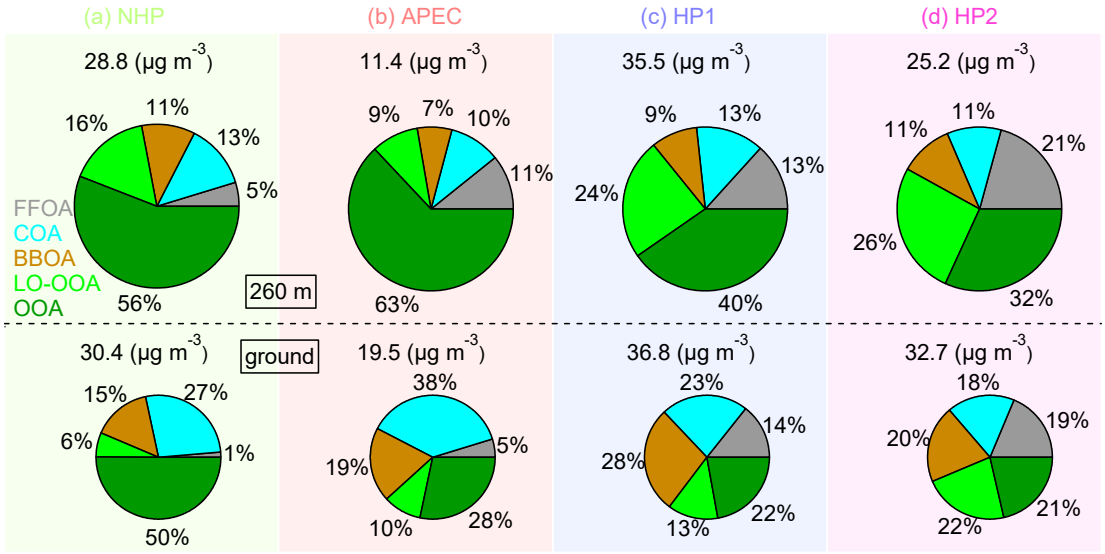

Figure 8: Average composition of OA during four different periods (a-d), i.e., NHP, APEC, HP1, and HP2. The OA factors resolved at ground site are also shown for comparisons (bottom panel).

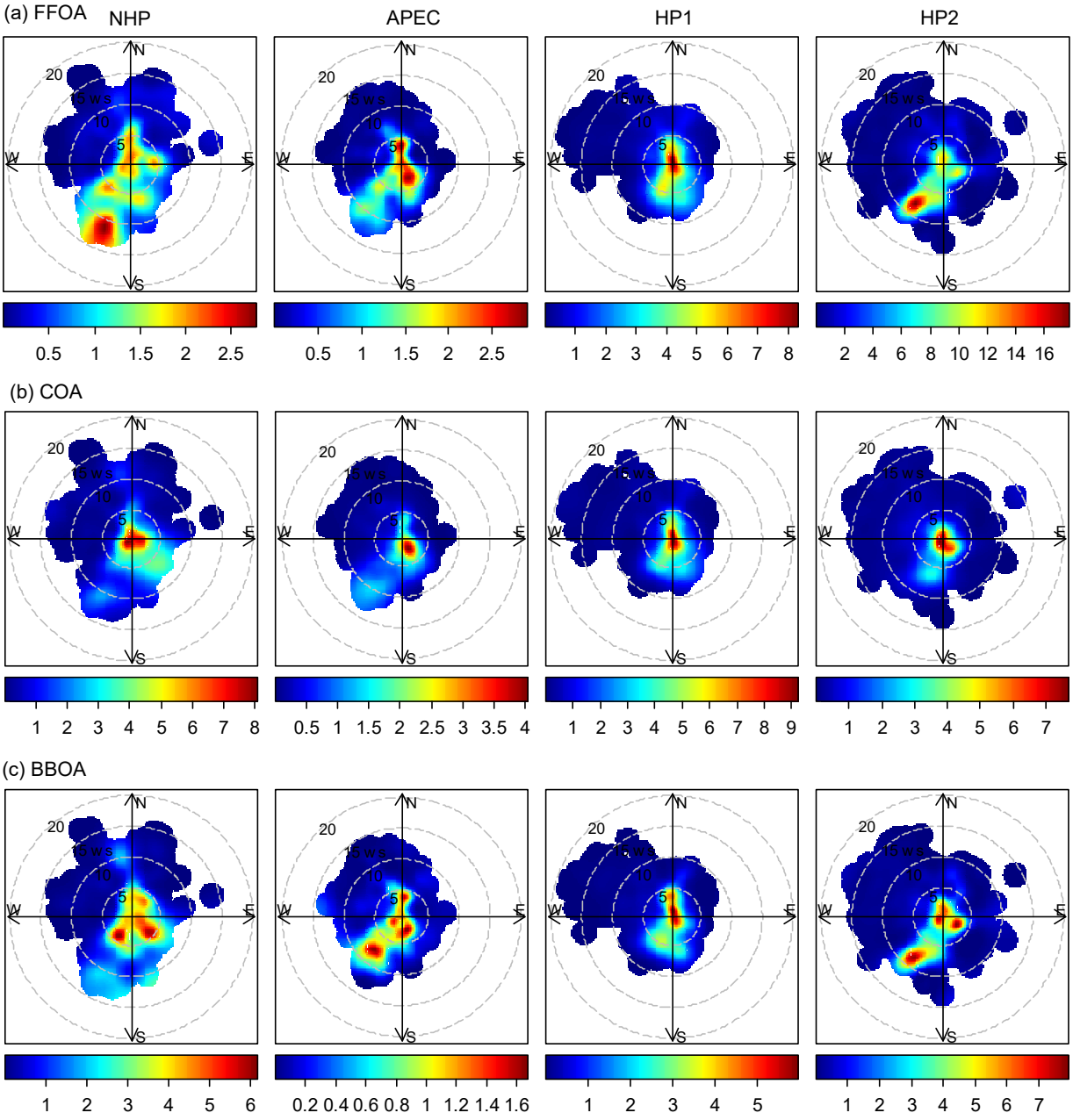
(a) FFOA
NHP
APEC
HP1
HP2
(b) COA
(c) BBOA
N
S
E
W
20
15 w s
10
5
0.5 1 1.5 2 2.5
0.5 1 1.5 2 2.5
1 2 3 4 5 6 7 8
2 4 6 8 10 12 14 16
1 2 3 4 5 6 7 8
0.5 1 1.5 2 2.5 3 3.5 4
1 2 3 4 5 6 7 8 9
1 2 3 4 5 6 7
1 2 3 4 5 6
0.2 0.4 0.6 0.8 1 1.2 1.4 1.6
1 2 3 4 5
1 2 3 4 5 6 7

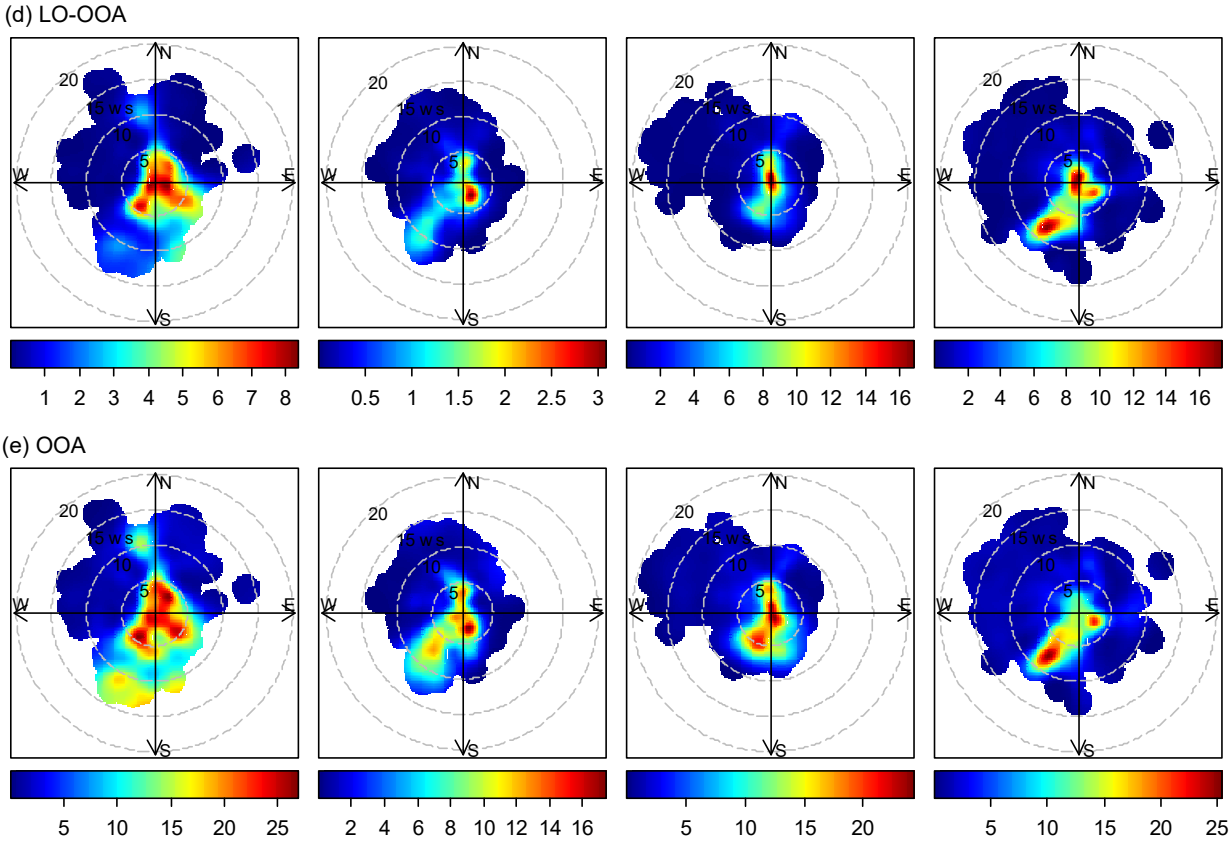

Figure 9: Bivariate polar plots of the mass concentrations of five OA factors (a-e) at 260 m as functions of wind direction and wind speed (m s^{-1}) during the four different periods.

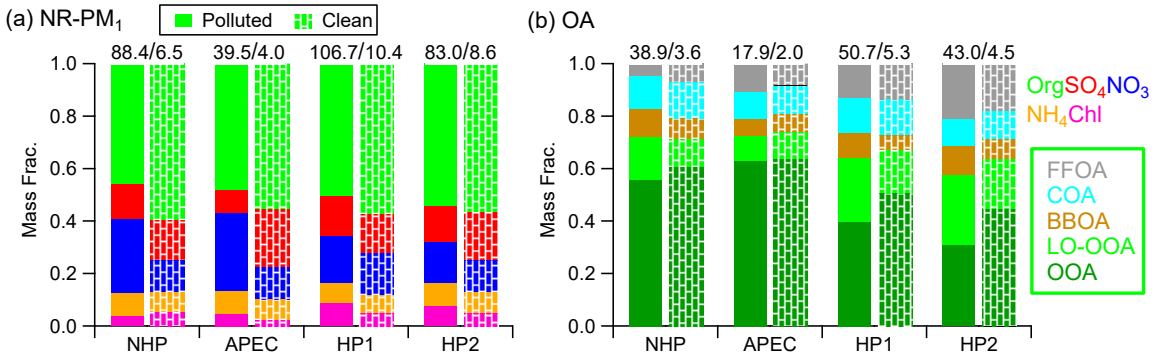

Figure 10: Comparisons of chemical composition of (a) NR-PM_1 and (b) OA between clean periods and polluted episodes that are marked in Fig. 1 during the four different periods, i.e., NHP, APEC, HP1, and HP2. The numbers on the top of the bar graphs are the average mass concentrations of NR-PM_1 and OA.

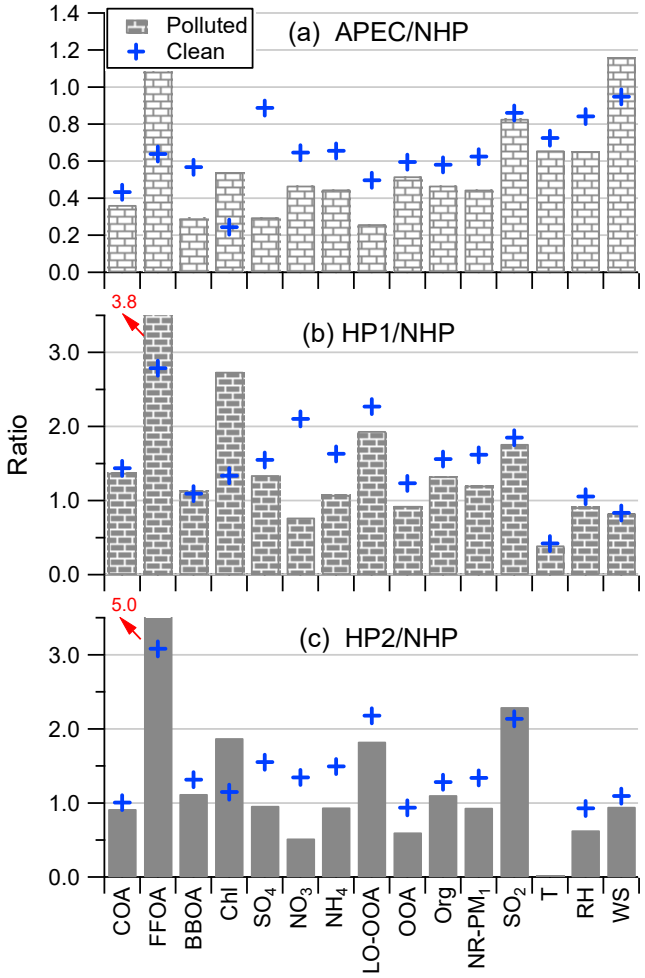

Figure 11: Comparisons of aerosol compositions, gaseous precursors, OA factors and meteorological variables between (a) APEC and NHP, (b) HP1 and NHP and (c) HP2 and NHP. All the data were separated into clean events and pollution episodes that are marked in Fig. 1.

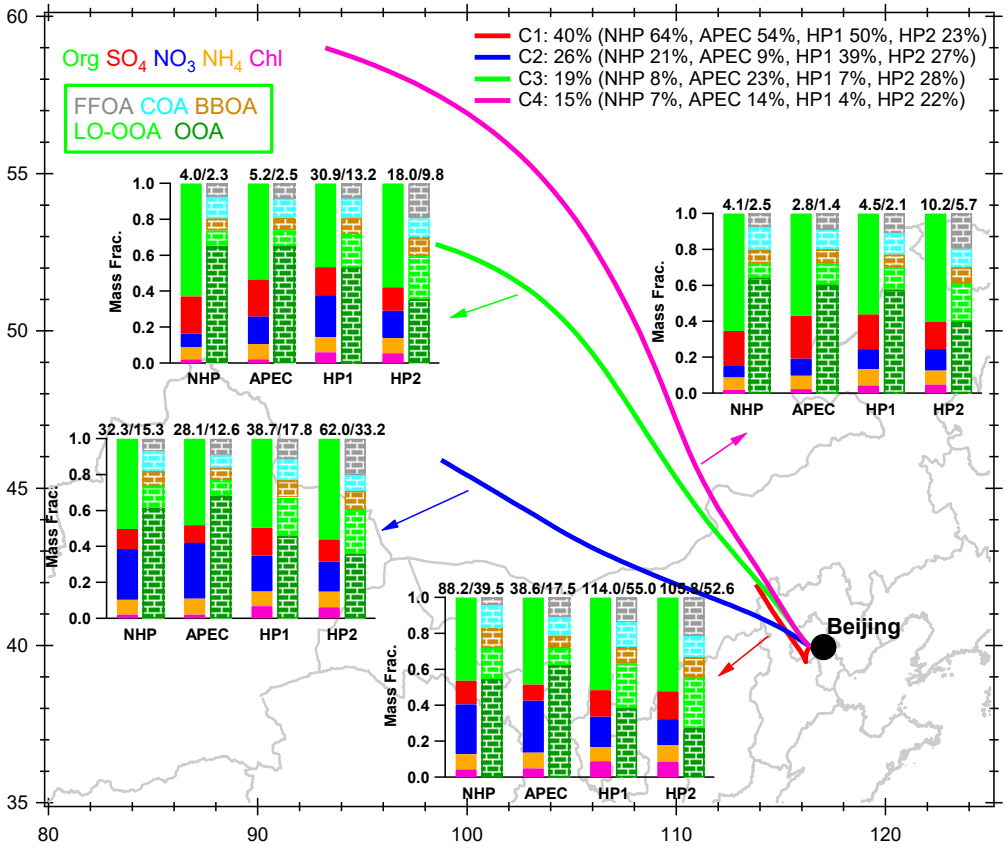

Figure 12: The average NR-PM$_1$ and OA composition for each cluster during the four different periods, i.e., NHP, APEC, HP1, and HP2. The numbers on the top of the bar graphs are the average mass concentrations of NR-PM$_1$ and OA. In addition, the number of trajectories and the corresponding percentages of the total trajectories are also shown in the legends.